Anandakumaran, Kanapathippillai

GROWTH AND PROPERTIES OF (TRANS 1,4-POLYISOPRENE) CRYSTALS

City University of New York PH.D. 1983

PLEASE NOTE:

In all cases this material has been filmed in the best possible way from the available copy. Problems encountered with this document have been identified here with a check mark ✓.

1. Glossy photographs or pages ✓
2. Colored illustrations, paper or print _____
3. Photographs with dark background ✓
4. Illustrations are poor copy _____
5. Pages with black marks, not original copy ✓
6. Print shows through as there is text on both sides of page _____
7. Indistinct, broken or small print on several pages _____
8. Print exceeds margin requirements _____
9. Tightly bound copy with print lost in spine _____
10. Computer printout pages with indistinct print _____
11. Page(s) _____ lacking when material received, and not available from school or author.
12. Page(s) _____ seem to be missing in numbering only as text follows.
13. Two pages numbered _____. Text follows.
14. Curling and wrinkled pages _____
15. Other _____

GROWTH AND PROPERTIES OF (TRANS 1,4-POLYISOPRENE) CRYSTALS.

BY

KANAPATHIPPILLAI ANANDAKUMARAN

A dissertation submitted to the Graduate Faculty in Chemistry in partial fulfillment of the requirements for the degree of Doctor of Philosophy, The City University of New York

1983

This manuscript has been read and accepted for the Graduate Faculty in Chemistry in satisfaction of the dissertation requirement for degree of Doctor of Philosophy.

9/28/83
date

Arthur E. Woodward
Chairman of Examining Committee

9/28/83
date

David C. Walker
Executive Officer

William E. L. Grossman
Supervisory Committee

The City University of New York

Abstract

GROWTH AND PROPERTIES OF (TRANS 1,4-POLYISOPRENE) CRYSTALS.

BY

KANAPATHIPPILLAI ANANDAKUMARAN

Adviser: Professor Arthur E.Woodward

Crystals of trans 1,4-polyisoprene in the α form were prepared from dilute amyl acetate solution employing the self seeding technique and crystallizing at T_C's of 10 to 34°C using fractions of Balata and Gutta Percha with $\bar{M}_n$ from $2x10^4$ to $4x10^5$ and $\bar{M}_w$ / $\bar{M}_n$ of 1.2 - 1.5. With a change of T_C from 10 to 30°C the lamellar thickness showed an increase from 78 to 125Å, the DSC endotherm increased from 58 to 68°C, the density changed from 0.96 to 0.98g cm^{-3} and the morphology changed from ellipsoidal to hexagonal. A similar effect in morphology and density was found on decreasing the $\bar{M}_n$ from 10^5 to 10^4.

The total noncrystalline fraction $1-W_C$ was determined from the density values and the surface fraction, F_S, for selected preparations by an epoxidation reaction. The epoxidation reaction was carried out on the crystals in amyl acetate suspension at 0°C as a function of time using m-chloroperbenzoic acid (MCPBA) until the reaction levelled off. It was found that crystal damage during the epoxidation reaction increases with increasing $\bar{M}_n$, (MCPBA), with increasing reaction time and with decreasing T_C . The number of monomer units per fold, calculated

from the epoxidation results was smallest for $\bar{M}_n = 2.4 \times 10^4$ (6) and showed an increase with increasing T_c at constant $\bar{M}_n$ (8 to 10).

ACKNOWLEDGEMENTS

I wish to express my sincere thanks to Professor Arthur E.Woodward for his invaluable guidence, extraordinary patience and deep understanding. His resourcefulness, constant encouragement and unwavering confidence in me made this project a very pleasant and rewarding experience.

At the same time, I would like to extend my gratitude to both Professors William E.L.Grossman and Nan-Loh Yang for their most helpful suggestions.

TABLE OF CONTENTS

LIST OF FIGURES

LIST OF TABLES

INTRODUCTION

When crystallization of a polymer is carried out isothermally from dilute solution, single folded chain lamellae of 50 - 200Å thick are usually formed[1-3]. The orientation of the chain molecules within the lamellae has been determined from selected area diffraction studies[2-3]. The patterns are usually extremely sharp and detailed analysis indicates that the chain axis is preferentially oriented perpendicular to the wide face of the crystal; moreover, the direction of the a and b crystallographic axis are preserved throughout the platelet structure so that the designation single crystals have been commonly given to such structures.

The study[4-5] of polymer single crystals is important to obtain knowledge concerning the disposition of chains within the crystals, the nature of the crystallization and melting processes (which are unusual in polymers), the special character of crystalline defects in these systems, and the effect of mechanical forces and temperature on polymer crystals. The understanding of single crystal structure is considered to be a necessary background for the study of polymers crystallized from the melt.

Measurements of properties such as (density, heat of fusion) conventionally used to determine the degree of crystallinity indicate a notable crystallinity deficiency in solution grown single crystals, which in the conventional

manner could be interpreted as an amorphous component. While some of the crystallinity deficit may be accountable by defects within the lattice, there is a general consensus of opinion that most of it is located along the fold surface. The nature of the fold region has been the subject of intensive study and controversy.

From the structural point of view the problem can be subdivided into the following separate questions. First, does the chain fold up along the crystal face or is it a completely random three dimensional switchboard[6-9] (Fig.1a), the latter automatically implying large amounts of fold looseness. Even in the case of chain folded sheets there are two further extreme alternatives, i.e. the folds can be adjacently reentrant or the stem reentry can be random on the average. Only in the case of adjacent reentry does the alternative of sharp, hence possibly regular folds, arise[10-13] (Fig.1b), on the other hand a distribution of fold stem lengths creates opportunities for loose folds[14-16] (Fig.1c).

Investigation of the crystalline content of dilute solution grown lamellae has been carried out using a variety of non destructive methods, which include (I) wide angle X-ray diffraction (II) density (III) calorimetry (IV) IR spectroscopy and (V) broadline NMR. A large number of these investigations have been on linear polyethylene. This literature has been reviewed by Mandelkern[17].

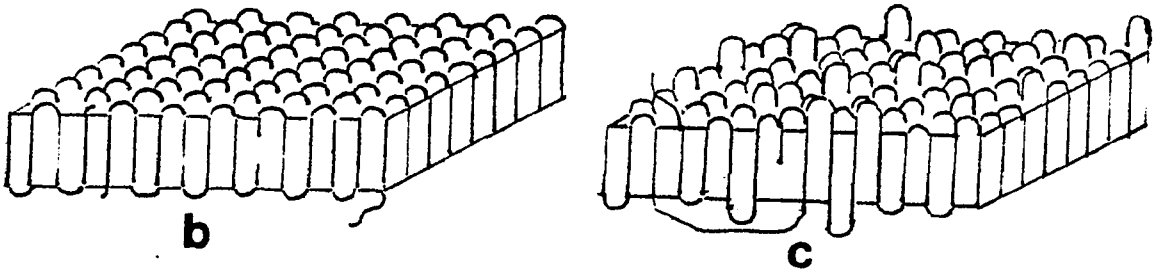

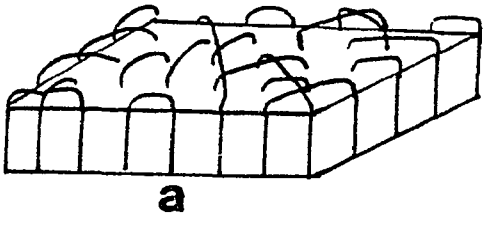

fig. 1 MODELS[4] OF CHAIN FOLDING IN SINGLE CRYSTAL LAMELLAE. (a) SWITCHBOARD (RANDOM ADJACENT RE-ENTRY) (b) REGULAR ADJACENT RE-ENTRY (TIGHT FOLD) (c) IRREGULAR ADJACENT RE-ENTRY (LOOSE FOLD).

For polyethylene crystals grown from xylene solution at relatively large super coolings and subsequent drying a disordered fraction of about 15-20% has been reported from heat of fusion measurements. But a disordered fraction of 11% has been found for crystals measured in silicon oil suspension[18]. This difference has been interpreted as due to the collapse of original hollow pyramids during drying, hence inducing lateral defects within lamellae. However in a similar[19] heat of fusion measurement experiment on dried samples and of the corresponding oil suspension samples the results agreed within the experimental error. Further the crystallinity derived from heat of fusion measurement, density or WAXS were found to be in excellent agreement. It has been reported[20], when the molecular weight of linear polyethylene is in the region of $2x10^4$ - $2x10^6$, the crystallite thickness is independent of chain length and depends only on the crystallization temperature for a given solvent. Bank and Krimm[21] showed that on oxidation of polyethylene single crystals with ozone the absorbance at 910 cm^{-1} which is due to the vinyl group falls rapidly to a constant low value suggests that the end groups are largely excluded from the interior of crystals.

Krimm et. al[21-22] used the mixed crystal technique containing mostly protonated polyethylene (PEH) and a small amount of deuterated polyethylene (PED) and analyzed the characteristic crystal field splittings in

the IR spectrum to determine the relative locations of chain stems of the PED molecule in the crystal lattice. In the IR spectrum, when PED stems were surrounded by first nearest neighbor PEH stems, internal modes (such as CD_2 bending and CD rocking) occured as singlet bands and when PED stems were located on adjacent lattice sites these bands were split due to interaction between nonequivalent stems. Experimentally, split bands were observed, hence the adjacent reentry model was supported for polyethylene single crystals. Mandelkern[23] attributed this splitting as due to significant aggregation of different PED molecules which would lead to a stem adjacency rather than the stem organization associated with a single molecule. In the recent experiments by Krimm et. al[24] segregation effects were eliminated using low PED concentration and large super coolings. On dilution of polyethylene with fully deuterated polyethylene, the intermolecular H-H coupling is replaced by the very small H-D coupling. Thus one can determine the intramolecular H-H coupling by extrapolation to infinite dilution. This intracoupling differs for different types of chain folding. It increases in the sequence of random reentry, adjacent reentry and molecular clustering. Using these differences on high resolution NMR Sillescu and Voekel[25] concluded that adjacent reentry folding with molecular clustering is predominant.

Udagawa and Keller[26] have found from the study of change of X-ray long spacing by swelling polyethylene single crystals with a liquid, that there is a disordered amorphous layer in the fold region which expands by swelling. The increase in long spacing was found to depend to minor extents on crystallization conditions such as concentration and crystallization temperature but increased very markedly with the molecular weight of the polymer in the region of $2x10^4$ - $1x10^6$. Mandelkern[27] has explained the dependence of the amount of swelling with molecular weight as being due to the variation of size and distribution of amorphous loops connecting the crystalline sequence.

Investigation of the material on the surface of dilute solution grown polyethylene lamellae available to penetration by low molecular weight liquids using broad line NMR have been reported by some investigators[28-30]. Values for this available material are 3-4% of the total and are much smaller than values for disordered content (5-20%) for polyethylene lamellae. Fisher[6] and Flory[8] measured the density of single crystal mats of polyethylene and found it corresponds to about 80 - 85% crystallinity i.e. about 15 - 20% of chains are disordered as compared to the 5% that is required to develop a regular fold structure. Hence they concluded in favor of random irregular polymer chain entry. To reconcile the higher amorphous content on a

regular folded model with adjacent reentry folding Hoffman et. al[31] have proposed that, noncrystalline chains are physically adsorbed at the lamellae surface and remain non crystalline following drying and temperature change. (see Fig.2).

Attempts have been made to study the fold region of polyethylene crystals directly by chemical assay but the degradative chemical reactions employed have resulted in destruction of the crystals themselves, and the results are difficult to interpret.

Digestion with strong oxidizing agents such as HNO_3 and destructive reaction with ozone coupled with gelpermeation chromatography has been used by Keller and coworkers[32-34] to obtain information about the distribution of fold lengths in polyethylene lamellae. In both the experiments two peaks in a 2:1 ratio dominated the chromatogram; it was concluded that the surface of the crystals consist of folds of various lengths and that some of the folds resided at different depths in the crystals. As the chains are cut at various locations, the peaks corresponding to longer chains decrease in intensity while those of shorter lengths increase. These experiments have been interpreted as confirming the model of adjacently reentrant folds of various lengths.

Substitution of bromine atoms onto polyethylene lamellae using ultraviolet or visible light activation

fig. 2 PROPOSED[31] MODEL WITH MOSTLY ADJACENT REENTRY FOLDING, CONSISTING OF PHYSICALLY ADSORBED POLYMER MOLECULES ON THE FOLD SURFACE.

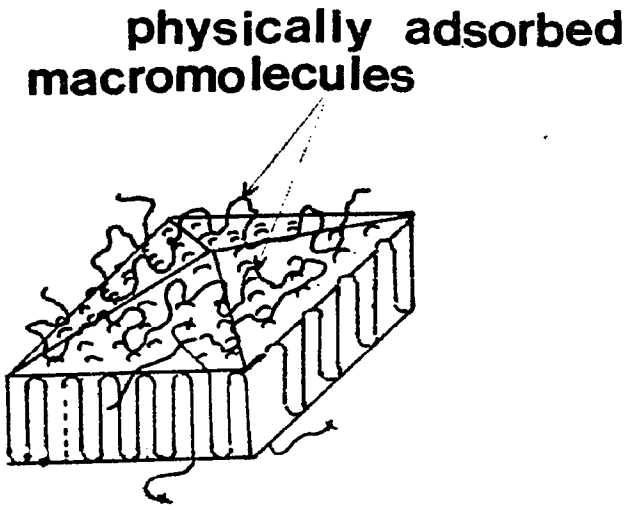

of Br_2 in solution at room temperature and above has been studied by various authors[35-38]. Harrison and Baer[36] report an initial fast reaction with a changing rate corresponding to about 2-3% bromine by weight; following that, the rate of bromine addition remains constant up to at least a 7% bromine content by weight. Assuming tight reentry folding, it was estimated that 4.5% bromine by weight corresponds to one Br atom per fold. In work using hydrogenated polyethylene Equiluz, Ishida and Hiltner[37] found that a constant value of 3.5% by weight bromine was reached at 40°C using Br_2 in bromobenzene under ultraviolet activation. In the above studies one crystal preparation grown at 93°C with thickness 170Å and the other grown at 65°C of 78Å thickness were used. Using Infrared C-Br stretching bands, the gauche/trans intensity ratio was higher for 93°C grown crystals than for 65°C grown crystals. This result has been interpreted interms of a tight fold mode of crystals formation for 93°C grown crystals and the presence of an amorphous layer or loose loops for the 65°C grown crystals. Substitution of chlorine atoms onto polyethylene lamellas using ultraviolet light activation of chlorine in solution at 7°C without apparent damage to the crystalline parts, as monitored by X-ray diffraction, was carried out for lamellas with four to thirty weight percent chlorine added[39]. A chlorine content of 26 weight percent corresponds to fourteen

monomer units per fold.

In carrying out studies of the amount of the crystalline and noncrystalline components in polymers, the use of diene polymers such as trans 1,4-polyisoprene (TPI) and trans 1,4-polybutadiene (TPBD), allows both chemical and physical techniques to be employed. The double bonds in the repeat units of TPBD react quantitatively[40-41], by reactions such as epoxidation therefore a reaction of this sort can be used to disclose the number of double bonds that are available for reaction at the fold surfaces of crystals in suspension, assuming that hidden folds are negligible and making corrections if necessary for chain ends excluded from crystallization. The knowledge of the number of double bonds available for the reaction can lead to an estimate of the tightness of the folds in various single crystals preparations if accurate data concerning the crystal structure and thickness of the crystals are known.

Dilute solution grown lamellas of (trans 1,4-polybutadiene) of high trans content have been investigated by various workers. A number of these studies have shown that the lamellas can possess a sizable noncrystalline component, the amount of which depends on crystallization conditions and annealing treatment. Two general methods have been employed in these investigations. One of these measures total noncrystalline

content regardless of its location in the lamellas, this type of measurement includes techniques such as density[42], X-ray[43], dynamical mechanical behavior[43], IR[44], Raman spectroscopy[45] and differential scanning calorimetry[46-48]. Hendrix, Whiting and Woodward[44] obtained IR spectra of TPBD crystal mats in the 1000-1400cm^{-1} region. It was found that the ratio of the intensity of the IR band at 1350 cm^{-1}, an amorphous band, to that at 1335cm^{-1}, a regularity band varies from 1.3 to 0.1 with the solvent used for crystal preparation, the TPBD used and with the thermal history. The ratio was found to decrease on annealing the crystal mat or when the crystallization temperature was increased. Ng, Stellman and Woodward[46] studied TPBD crystals using DSC. Here ΔH_t, the heat of transition, for the conversion of the low temperature modification to high temperature modification was assumed to be proportional to crystallinity. These results were in agreement with that of the results obtained by IR measurements. Tseng et. al[42] extrapolated the straight line obtained by plotting the enthalpy of crystal - crystal transition versus specific volume to 100% crystallinity and obtained a value for the heat of fusion of TPBD, in agreement with the literature value. The other general method measures only the amount of those disordered parts of the lamellae which can be reached by penetration from the surface

either by chemical reactants (epoxidation[40-42,49] bromination [40,50], OSO_4 treatment[48]) or by low molecular weight liquids which enhance polymer chain mobility[43,51] (broad line NMR). The total amount of amorphous material in a solid can be estimated using broad line nuclear magnetic resonance. If conditions are such that some reorientation motion is taking place in the amorphous component and the crystalline region are effectively rigid, then a two component NMR absorption will be found, the narrow part being associated with the mobile region. In the presence of solvent, which can only penetrate the amorphous region and can greatly enhance the narrow line, both the crystalline and the amorphous resonances were observed more clearly. For some TPBD preparations[51] using this technique the total amorphous content exceeded that present at the crystal surface region alone, as determined using other methods (IR and DSC), which implied that amorphous regions do exist in the interior of the crystals too. Woodward and coworkers[40] carried out an epoxidation reaction of the single crystals of (trans-1,4-polybutadiene) in suspension in the 6-21°C range with samples having number average molecular weight 36,000 and 5500. The fraction of double bonds reacted with the epoxidizing agent meta-chloroperbenzoic acid (MCPBA) was obtained by monitoring the IR intensity ratio of the carbonyl absorption for MCPBA (1700 cm^{-1}) and meta-chlorobenzoic acid MCBA (1735 cm^{-1}). The experimentally determined average number of monomer

units per fold, for heptane and toluene grown crystals ($\bar{M}_n$ = 36,000) were 2.4 and 5.6, respectively, and 4 for heptane grown crystals of $\bar{M}_n$ = 5500.Comparing the above values with the theoretically estimated values for possible tightest reentrant fold it has been concluded that TPBD ($\bar{M}_n$ = 36,000) crystals grown from heptane principally contain regular reentrant folds and TPBD crystals grown from toluene contain irregular adjacent reentrant folds. Also the increase in the % double bonds available for epoxidation with the decrease in $\bar{M}_n$ was postulated to be due to the larger number of chain ends or cilia at the surfaces.

Recently Tseng et. al[42] estimated the average number of monomer units per chain end to be $\frac{.79L}{2}$ /R by analyzing the epoxidation results of eight TPBD preparations obtained by crystallization from dilute heptane and in one case from toluene solution. Here L is the lamellar thickness and R the repeat distance of a monomer unit along the polymer chain. The crystal preparations had $\bar{M}_n$ values of 4700 to 1.2×10^5 and $\bar{M}_w / \bar{M}_n$ of 1.3 to 2.7. The total noncrystalline content was determined by density measurements and the amorphous content on the surface was obtained by analyzing the epoxidized samples using ^1H NMR. In the above studies the number of monomer units per fold was found to decrease with the crystallization temperature and to a lesser extent with molecular weight. Schilling et. al[52]

analyzed two epoxidized samples from the above preparations employing ^{13}C NMR spectroscopy. From the intensities of junction methylene carbon resonances between runs of epoxidized and unreacted monomer units, the fold length and crystalline stem lengths were calculated. The stem length obtained by this method was in agreement with LAXS measurements and the fold length was found to be 2.5 - 3.0 monomer units corresponding to the tightest possible fold.

Only a few studies of dilute solution grown crystals have been reported[53-54] for trans 1,4-polyisoprene. This polymer exist in two known crystalline phases, one with an orthorhombic unit cell[55] (β form) and other a monoclinic unit cell[56-57] (α form). In both the crystalline forms four long chain molecules pass through the unit cell parallel to the C axis and composed entirely of either right or left, handed molecules. The difference in the stereo structures are attributed[55] to the positions of the single bonds CH_2 - CH_2 which join the isoprene units together in the crystalline natural rubber also four chains pass through the unit cell but two are right handed chains and the other two are left handed chains. The unit cell parameters determined by X-ray diffraction on melt crystallized samples of β form[55] are a = 7.83 Å b = 11.87 Å c = 4.75 Å, $\alpha = \beta = \gamma = 90$ and of α form[57] are a = 7.98 Å, b = 6.29 Å c = 8.77 and $\beta = 102$. As

proposed by Bunn[55], Fisher[56] reported the existence of a third form (γ) with unit cell parameters a = 5.9Å , b = 7.9Å, c = 9.2Å and γ = 94, by using the electron diffraction datas of the unoriented and the preferred oriented samples. However using the X-ray diffraction patterns of the sample obtained under the same condition as in Fisher's work Takahashi et. al[57] concluded that the spacings of the γ form reported by Fisher correspond to those of the α form, although the unit cell parameters (a and b) reported by Fisher was not same due to different indexing.

In the preparation of TPI crystals from dilute solution under conditions reported[54] earlier, mixtures of α and β were usually obtained although it was found possible to prepare samples of either one form or the other. For bulk and for dilute solution crystallized TPI, α melts at a higher temperature than β[58]. However the highest melting point observed to date is for β prepared by stirrer crystallization[59]. According to Mandelkern et. al[58] the β phase is metastable and it converts to the α phase by a process of fusion and crystallization. No solid-solid transformation has been observed. This melting and recrystallization process with and without diluent added has been studied by other workers[53,58-63]. The β to α change has been reported[53] as taking place at room temperature in the presence of a suitable liquid . When TPI was

crystallized from the melt and examined under crossed nicols, two types of spherulites were observed[64-65]. Spherulites displaying characteristic maltese cross were identified with the β form and the dendritic spherulites were found to be of the α form. Melt crystallized cis 1,4-polyisoprene, also exhibits two melting endotherms. This was found to be due to two different morphological forms, but with the same crystal structure[66-67]. Some authors[63,68-72] attempted to fractionate TPI in to sharp fractions. But the polydispersity of the fractions obtained were usually in the region of 1.5 for lower molecular weight and higher for higher molecular weight samples.

The Objectives of the Proposed Research.

The principal goal of this research is the determination of the amount and general location of the non-crystalline components associated with dilute solution grown crystals of (trans 1,4-polyisoprene) as a function of molecular weight. To meet this goal the following were carried out:

1) Preparation of crystals from dilute solution using sharp molecular weight fractions.
2) determination of the interfacial fraction of dilute solution grown crystals as a function of molecular weight.
3) determination of the total non-crystalline fraction of dilute solution grown crystals as a function of molecular weight.
4) determination of the average fold length for dilute solution grown crystals as a function of molecular weight.

EXPERIMENTAL

Samples:

Synthetic trans-1,4-polyisoprene (polysciences Inc) Balata (Dunlop) and Gutta Percha (Gabundan Produsen Karet, Indonesia) were used.

Characterization:

The trans-(1,4) content was determined as 99 and 100% respectively for samples of synthetic polymer and Balata which had been crystallized from amyl acetate solution at a polymer weight fraction of 5.7×10^{-4}. These determinations were made by F.A.Bovey and F.C.Schilling at Bell Laboratories by ^{13}C NMR using a Varian XL 200 instrument. The molecular weight distribution for each sample was obtained with a Waters 200 analytical GPC with toluene at 85°C as the solvent; calibration was carried out with five polyisoprene standards in the 1.0×10^4 to 8.0×10^4 range, two polybutadiene standards with weight-average molecular weights of 1.0×10^3 and 2.7×10^3, and squalene (molecular weight 411). For molecular weight above 8.0×10^4 an extrapolation of the results for the polybutadiene and polyisoprene standards was made, paralelling the curve obtained from a series of polystyrene standards. The GPC scan for squalene yielded $\bar{M}_w / \bar{M}_n = 1.06$, therefore 0.06 was subtracted from the $\bar{M}_w / \bar{M}_n$ values obtained from the GPC curves for each of the TPI preparations as a boundary spreading correction.

The $\bar{M}_n$ and $\bar{M}_w$ / $\bar{M}_n$ of unfractionated samples were:

Synthetic TPI	$\bar{M}_n$	= 3.5×10^4	$\bar{M}_w$ / $\bar{M}_n$	=	4.8
Balata	$\bar{M}_n$	= 1.1×10^5	$\bar{M}_w$ / $\bar{M}_n$	=	2.2
Gutta Percha	$\bar{M}_n$	= 6.3×10^4	$\bar{M}_w$ / $\bar{M}_n$	=	4.3

Fractionation:

A. Fractions of Balata TPI were prepared by fractional precipitation from toluene solution with methanol, where a solution of Balata 1% (W/V), deoxygenated by bubbling with dry N_2 was treated with methanol and stirred well until a milkyness developed at room temperature. The resulting mixture was warmed to about 40°C with constant stirring to homogenize the precipitate and an additional volume of methanol was added, this was kept over night in an isothermal bath at 28°C. The separations were observed to involve two liquid phases as required. The supernatant phase was removed, a further increment of methanol was added and the process was repeated. The liquid like precipitate was completely precipitated by adding excess methanol, filtered, dried under vacuum and subjected to GPC analysis.

B. Gutta Percha sample was fractionated on a diatomaceous earth column[73] (see Fig.3) with amyl acetate as the solvent and 2- ethoxyethanol (cellosolve) as the nonsolvent at 64°C in the presence of 2,2' methylenebis (4-methyl-6-tert-butyl) as antioxidant. This technique has some advantage over the fractional

precipitation technique, since the amount of solvent required for each fractions can be controlled, hence will result in sharp fractions. This column is supported on a medium porosity glass frit and the entire column is surrounded by a jacket in which the vapors of the heating liquid (methanol B.pt 64°C) are refluxing. Here 1% (W/V) polymer solution was poured onto the celite packed column which was heated above the polymer melting point 64°C and was allowed to deposit by crystallization as the column cools to room temperature. The polymer packed column was washed with enough cellosolve to remove all the solvent in the column before extraction. The column was always kept wet with solvent or non solvent. The solvent non-solvent mixture was added dropwise through the solvent reservoir which has been heated to 60-64°C using a heating tape. By increasing the solvent ratio, different fractions were collected at 64°C. Approximately 4 to 5 liters of solvent/ nonsolvent mixture was used to collect each fraction. Sometimes this amount was not sufficient; however even in those cases the solvent ratio was changed, but the initial liter of solvent plus polymer was discarded. Each one liter solvent/ non-solvent mixture with the polymer was collected separately and precipitated. GPC curves were obtained only for the final 1 liter collection of each fractions.

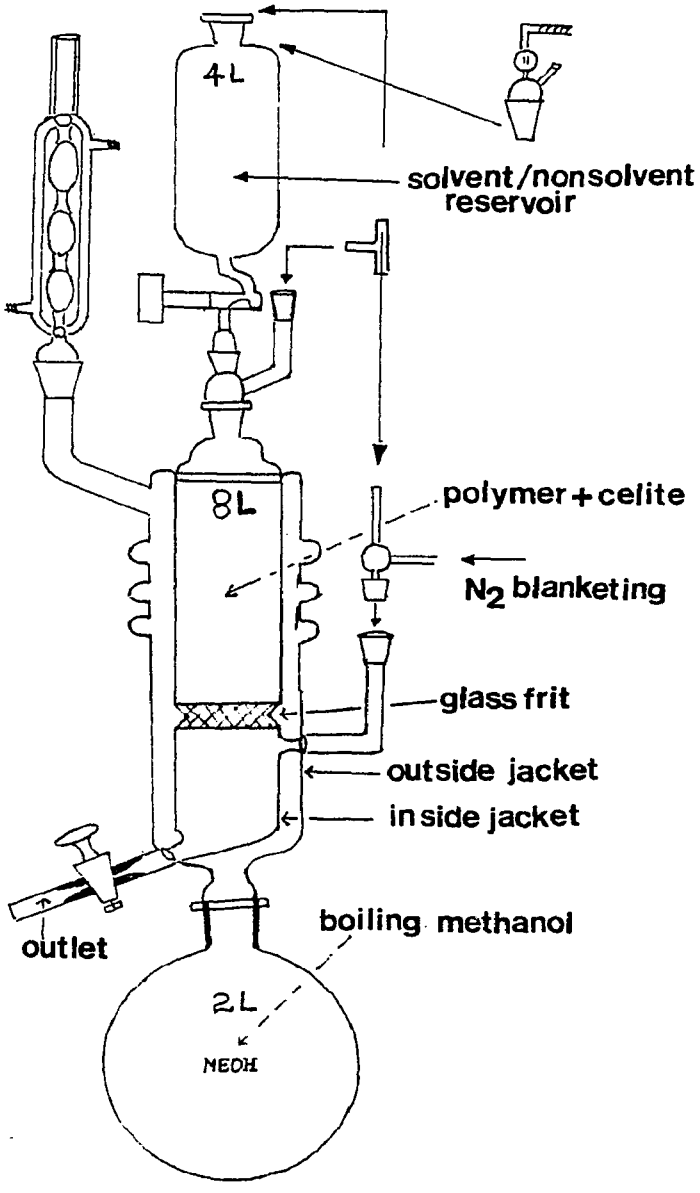

FIG. 3

DIAGRAM OF FRACTIONATION COLUMN

Crystal Growth Technique:

The technique used involves dissolution (T_D), precipitation at 0°C, heating to a temperature T_R, that caused disappearance of the precipitate for high molecular weight polymer and crystallization at T_C. Sometimes T_R was changed or directly crystallized from T_D to T_C. A weight of .05gm of polymer was dissolved (T_D) at 75°C in a flask which contained 100ml of amyl acetate. The solution was filtered and precrystallized at (T_p) 0°C. Then slowly heated (ca 1°C/ min) to a temperature (T_R) 40°C, finally crystallized at constant temperature T_C from 10 to 34°C. Crystallization over night appeared complete. The crystal suspension was filtered and washed with amyl acetate at T_C. The mats were then either dried at room temperature for density measurements and for X-ray diffraction or resuspended for epoxidation.

Crystal Morphology:

Crystals were deposited from suspension on to a copper grid which was coated with carbon. The grid was then shadowed with Pt - Pd for better contrast. The crystals were observed using a Phillips EM 300 operating at 80 KV; usually the magnification was in the range of 10,000 to 25,000 times. Pictures of crystals were taken directly with a plate camera attached to the electron microscope.

Epoxidized crystals were also observed under the electron microscope as a function of epoxidation time to monitor possible changes in surface morphology. These crystals were deposited on the grid after several washings with fresh cold amyl acetate.

Lamellar Thickness:

Lamellar thickness was determined using electron microscopy, on Pt - Pd shadowed samples at an angle of $\tan^{-1} 1/3$, by measuring the shadow length. The magnification was usually in the region of 40,000 to 90,000 times.

Density Measurements:

Densities were determined using a density gradient column at room temperature. This column was set up by mixing various proportions of heavy (water) and light (ethanol) solvents, so that the density in a glass column increases linearly from top to bottom. The gradient was calibrated using glass beads of known density. The gradient is sensitive to the fourth decimal of density and stable over night. All samples were pressed at 3.4×10^7 Pa to eliminate air. The weight fraction of the noncrystalline component $1-W_c$ was calculated (Eq 1) assuming a two phase system using an amorphous density[60] ρ_A of 0.905g cm^{-3} and a crystalline density[57] ρ_c of 1.05g cm^{-3}.

$$W_c = \frac{\rho_c [\rho_s - \rho_A]}{\rho_A [\rho_c - \rho_A]}$$

Equation - 1

Electron and X-ray Diffraction:

Electron diffraction was done on unshadowed specimens using the Phillips EM 300 instrument. The specimen was searched at very low beam current; when a diffraction pattern was seen, the beam current was increased and photographed. The diffraction area was also examined at a higher intensity in transmission to confirm the presence of a crystal after obtaining the diffraction pattern.

Wide angle X-ray diagrams were obtained with a cylindrical camera of 57.3mm diameter, for crystal mats which were pressed to disorient the system.

Differential Scanning Calorimetry:

Measurements were made with a Dupont 990 thermal analyzer with sample weights of approximately 2mg; all the runs were made at a rate of 10 °C/min. The apparent melting points were taken as the endotherm temperatures, after the zero correction for each run.

Epoxidation Experiments:

Reaction of the double bonds at the crystal surfaces $(TPI)_o$ ca .1gm per 100ml solvent was carried out in amyl acetate suspension at 0°C with enough m-chloroperbenzoic acid being added to the liquid phase to react with at least 70-80% of the double bonds in the polymer samples initially crystallized. Two procedures for adding the MCPBA were used: either all was added at the beginning of the reaction or half was added then and half after seven days. For most of the epoxidations (MCPBA) was 0.2gm per $100cm^3$ solvent although concentrations as low as 0.1 and as high as 1.0g per $100cm^3$ were used. The progress of the reaction was followed with time. After recovery of the epoxidized crystals, (unreacted MCPBA and the by-product MCBA was removed by washing with cold amyl acetate and finally with cold ether) they were freeze dried, dissolved in deuterated chloroform (ca 10% W/V) and subjected to ^1H NMR using a JEOLCO JNM MH 100. The CH, CH_2 and CH_3 resonances for TPI are found[74] at 5.1, 2.0 and 1.6 ppm and for epoxidized units they are at 2.7, 1.6 and 1.3 ppm. The fraction epoxidized was generally determined using the areas under the CH resonance peaks and the CH_3 resonance peaks, although in a few cases only the first was used. For the calculation from the CH_3 resonance peaks the following equation was employed.

$$F_S = 3A_5 / (3A_4 - A_5) \qquad \text{Equation-2}$$

A_5 is the area under the resonance at 1.3 ppm and A_4 the area under the resonance at 1.6 ppm. The relative intensities of the signals in the ^1H NMR spectra were determined by cutting out and then weighing each peak in the xerox copies of the spectra.

The above standard method of calculating the amount of epoxidation was confirmed by quantitatively epoxidizing TPI in chloroform solution to various amounts of epoxide content and analyzing the product by NMR using the above equation. Here TPI was dissolved in chloroform (.68gm in 100ml $CHCl_3$) at room temperature, meta-chloroperbenzoic acid was (MCPBA) added while stirring the solution at 20°C to give a product with epoxide content of 25% or 30%. After 5-6 hours a precipitate was obtained by adding the reaction mixture to methanol at 5°C. Finally the precipitate was filtered washed well with fresh methanol, cold ether at 5°C and dried over night under vacuum.

Squalene (a model compound of TPI) was also epoxidized in $CHCl_3$ at 0°C with MCPBA to various contents. The product was purified[75-76] by extracting with 5% cold sodium hydroxide dried over anhydrous sodium sulfate, filtered and the solvent removed at room temperature.

RESULTS

1. FRACTIONATIONS:

Molecular weight distribution curves from GPC are given in Fig. 4 for Balata samples obtained by the fractional precipitation technique. Molecular weights and polydispersity values derived from these curves are given in Table I. From this technique low molecular weight fractions were not obtained possibly due to the very high solubility in toluene.

Table. I. Value of $\bar{M}_n$, $\bar{M}_w$ / $\bar{M}_n$ of Balata Fractions

Sample	$\bar{M}_w$ / $\bar{M}_n$	$\bar{M}_n$
Balata (unfrationated)	2.2	1.1×10^5
Fraction #1a	1.5	3.8×10^5
Fraction # 1b	1.4	2.8×10^5
Fraction # 1c	1.3	2.3×10^5
Fraction # 2	1.4	1.1×10^5
Fraction # Y_1	1.4	2.9×10^5

Since one of the goals of this research was to obtain sharp polymer fractions over a wide molecular weight range, the column chromatograpic technique

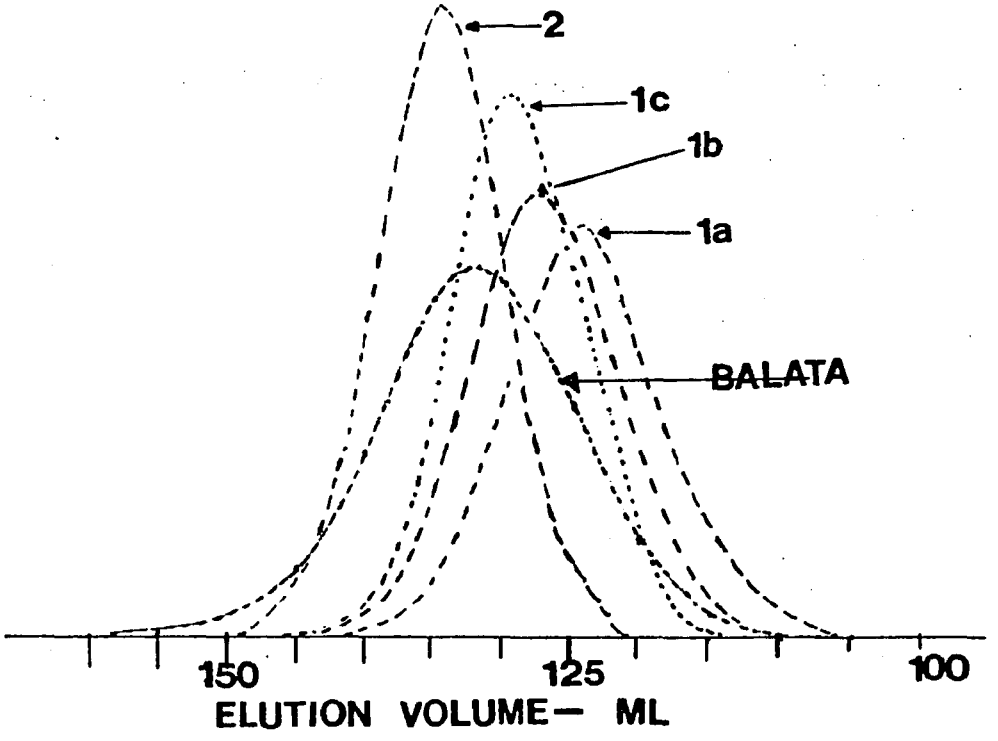

FIG.4 Gel permeation chromatograms for BALATA fractions

was chosen for the separation of Gutta Percha. The GPC curves of the different fractions obtained from Gutta Percha are given in Fig.5; Table II summarizes the results of the fractionation in terms of yield, molecular weight and dispersity. By comparing the GPC curves of the highest molecular weight fractions with the curve for the unfractionated sample, it is clear that a high molecular weight portion was not removed from the column. Also, when the column was cleaned, a white precipitate was found adhering to the celite surface even when pure amyl acetate or toluene was used to elute the column at 64°C. The GPC curves for the fractions eluted initially indicate the absence of degradation of this polymer during the course of the separation. Here the interference from crystallinity was avoided by averaging out the separation above the melting point of the polymer.

2. GROWTH of α CRYSTAL Form.

Samples of TPI (Balata, Gutta Percha and synthetic) obtained from amyl acetate solution after dissolution at 75°C by cooling to 0°C (T_p) followed by heating to 40°C (T_R) and crystallization at constant temperature T_C from 10 to 34°C yielded one crystal form only as evidenced by the appearance of a single

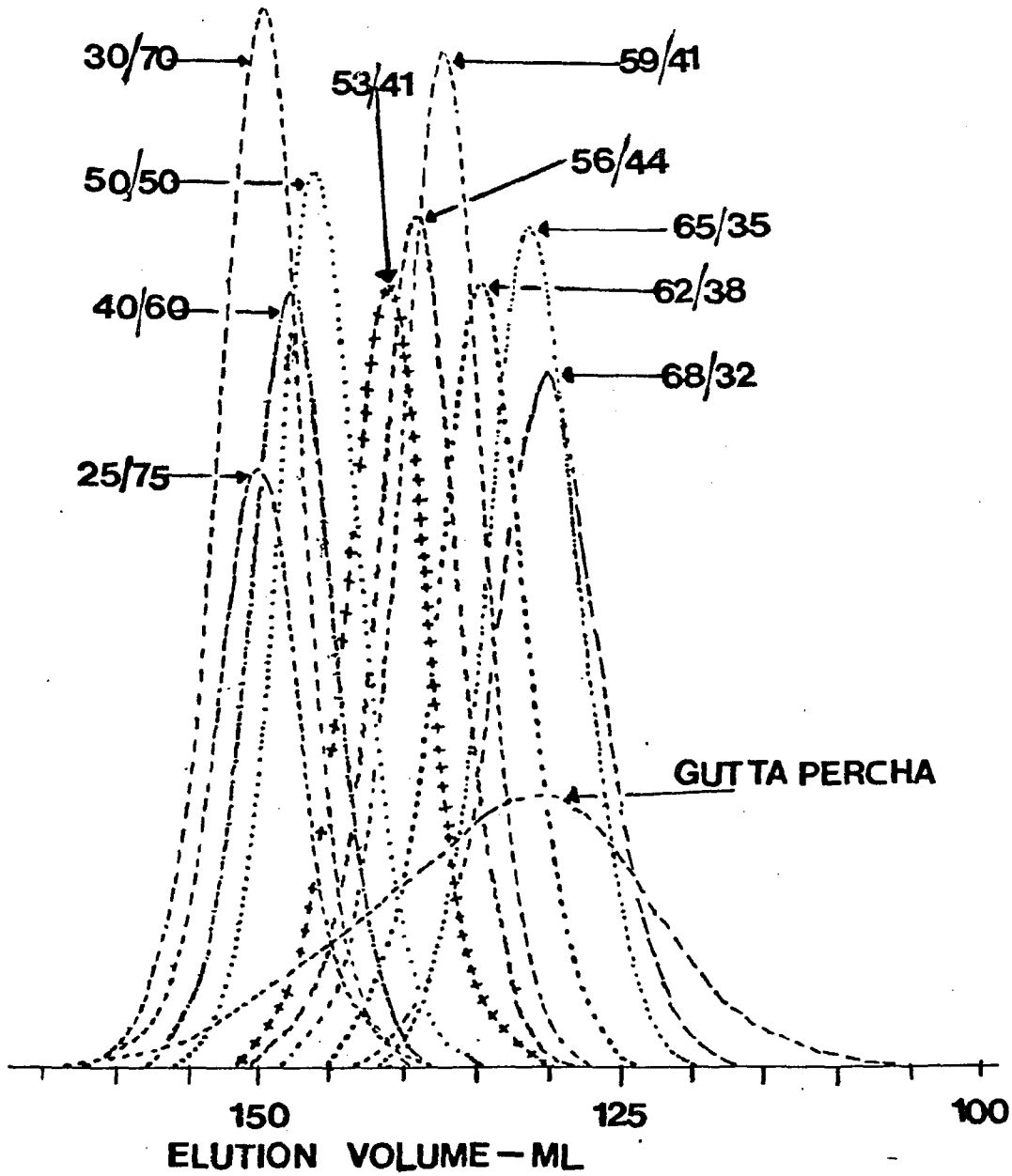

FIG.5 Gel Permeation Chromatograms for GUTTA PERCHA fracactions

Table II

Value of $\bar{M}_n$, $\bar{M}_w / \bar{M}_n$ of Gutta Percha Fractions

Solvent NonSolvent Ratio (V/V)	Weight of Fraction (g)	% of Total	$\bar{M}_n$	$\bar{M}_w / \bar{M}_n$
30/70			1.2×10^4	1.2
35/65			1.5×10^4	1.3
40/60	0.9	3.75	1.9×10^4	1.2
45/55	1.3	5.4		
50/50	1.5	6.3	2.6×10^4	1.2
53/47	1.2	5.0	4.1×10^4	1.2
56/44	1.7	7.1	5.4×10^4	1.2
59/41	2.3	9.6	6.9×10^4	1.2
62/38	3.2	13.3	1.0×10^5	1.2
65/35	2.5	10.4	1.6×10^5	1.2
68/32	2.5	10.4	2.1×10^5	1.3
70/30	0.4	1.7		

DSC endotherm as seen in Fig.6. For a polymer weight fraction of 5.7×10^{-4} an increase in T_C from 10 to 34°C, leads to an increase in the endotherm temperature from 58 to 69°C as shown in Table III. Endotherms in this region have been previously identified[54,63] with α TPI. This finding was confirmed in this work by carrying out wide angle X-ray diffraction on samples having T_C's of 0, 10, and 20°C. The diffraction patterns obtained were characteristic of the α form. Details of the spacings observed are given in Table IV together with the published[56] data. However a small amount of β form was present in the 0°C preparation as evidenced by a secondary, DSC endotherm at 48°C as seen in Fig.7. Figure 8 is a typical selected area diffraction pattern obtained for single crystals grown at a T_C of 20°C (T_R = 40°C), which can be indexed using the monoclinic unit cell proposed by Fisher[56]. Similar patterns were obtained at a T_C of 30°C and with low molecular weight fractions with T_C's of 20°C or 30°C.

3. EFFECT of REDISSOLUTION TEMPERATURE on CRYSTAL Form

The minimum temperature at which TPI heated to 75°C and then precipitated at 0°C would redissolve was found to be 40°C when $\bar{M}_n$ is 1.1×10^5 to 3.8×10^5. As shown in Table III T_R values of 40, 45 and 50°C were also used. When selected area diffraction

fig.6

DSC ENDOTHERMS OF α TPI CRYSTALS GROWN FROM DILUTE AMYL ACETATE SOLUTION

$\bar{M}_n = 2.9 \times 10^5$ $T_R = 40°C$ (a) $T_C = 20°C$, (b) $T_C = 30°C$.

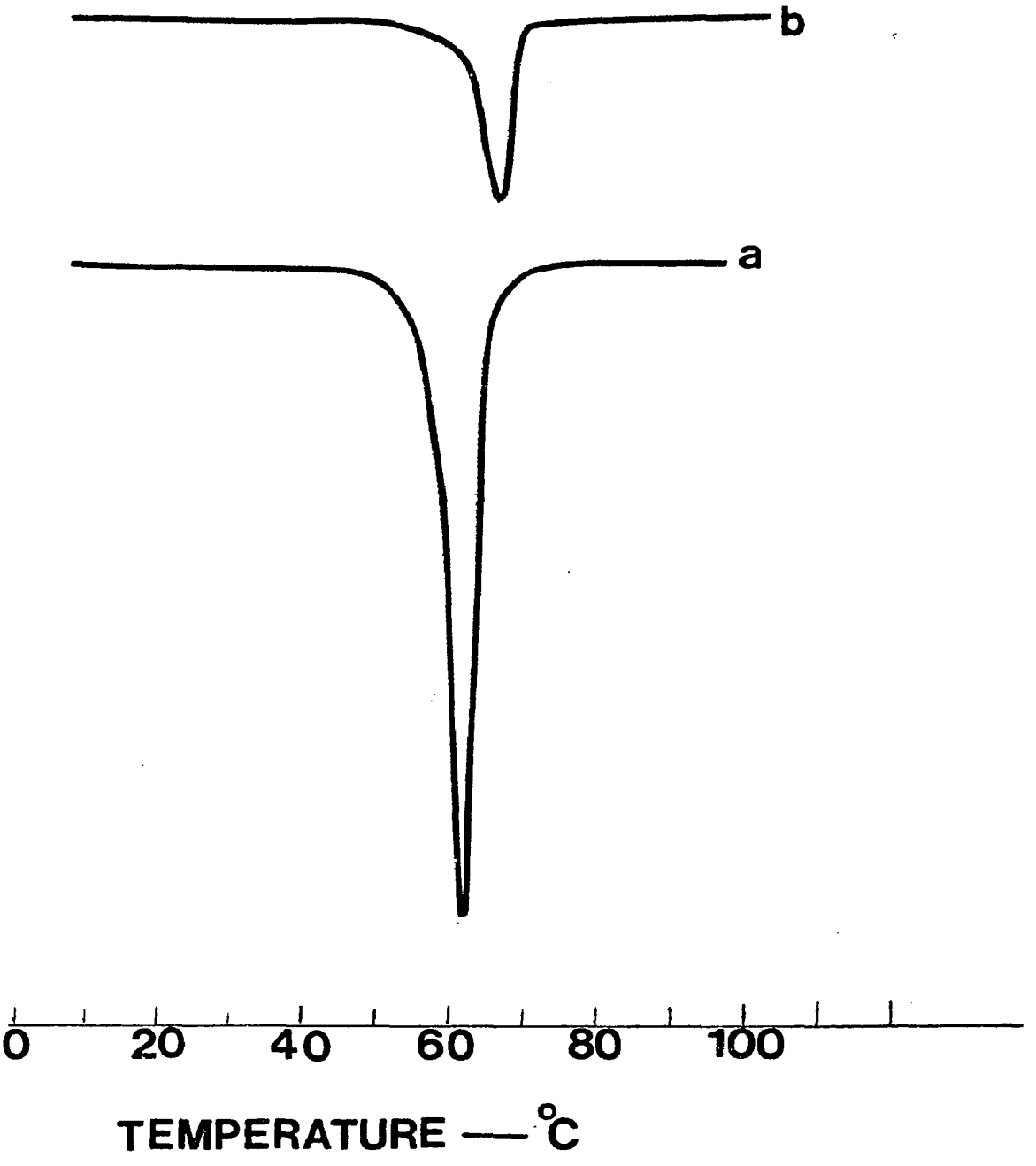

Table III

Crystallization of α TPI from Dilute Amyl Acetate Solution.

$\bar{M}_n$	$\bar{M}_w / \bar{M}_n$	T_R (°C)	T_C (°C)	DSC Endotherm (°C)
3.8×10^5	1.5	40	32	68
		40	30	68
		40	25	64
		40	20	63
		45	20	63
		50	20	63
		40	10	60
2.8×10^5	1.4	40	32	68
		40	30	66
		40	20	62
		40	10	60
2.9×10^5	1.4	40	34	69
		40	32	68
		40	30	67
		40	25	64
		40	20	63
		40	10	58
		50	20	63[a]
		40	0	48,56,63[b]
2.3×10^5	1.3	40	20	63
1.1×10^5	1.4	40	20	63
		40	10	58
0.69×10^5	1.2	40	20	60
0.26×10^5	1.2	40	20	61
0.19×10^5	1.2	40	20	60

a. Electron Diffraction Shows Predominantly β Form

b. X-ray Diffraction Shows Predominantly α Form.

Table IV

Comparison of Observed d-Spacings with Literature[56] Values for α Form

d-Observed (Å)		d-Literature (Å)
7.78	m	7.91
4.82	vs	4.95
3.90	vs	3.95
3.36	vs	3.36
3.02	mw	2.95
2.78	mw	2.73
2.30	vw	2.40
2.08	w	2.29
1.92	vw	2.03

w - weak

m - medium

s - strong

fig. 7 DSC ENDOTHERM OF TPI CRYSTALS GROWN FROM DILUTE AMYL ACETATE SOLUTION.

$\bar{M}_n = 2.9 \times 10^5$ $T_R = 40°C$, $T_C = 0°C$

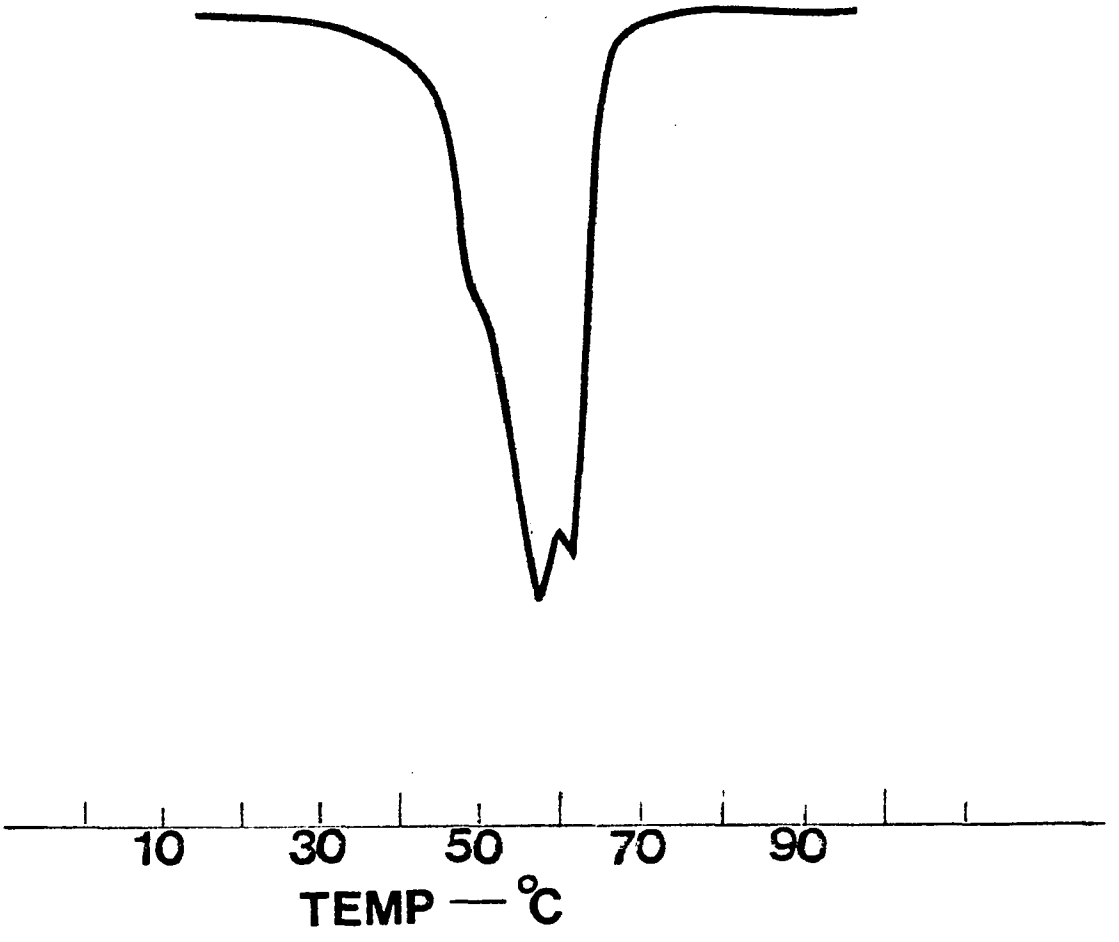

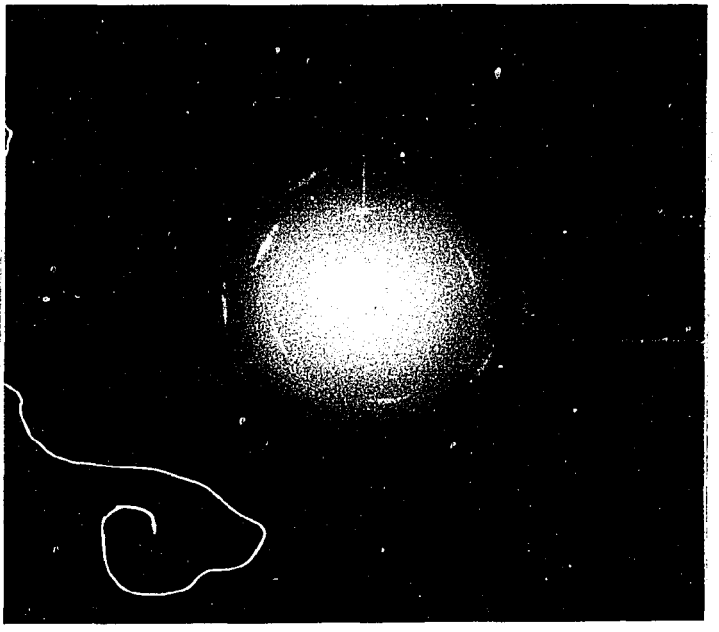

Fig.8 Selected area diffraction pattern of a single crystal of the α form of trans 1,4 polyisoprene, grown from dilute amyl acetate solution.
$\bar{M}_n = 2.9 \times 10^5$, $T_R = 40℃$ qnd $T_C = 20℃$

was carried out on individual crystals with T_R = 50°C and T_C of 20°C, the β TPI pattern was the only one observed as shown in Fig.9. However filtering and then drying at room temperature for two days yielded a dry mat showing principally the α crystalline form on X-ray diffraction analysis. Crystallizing with T_R of 50°C at a T_C of 0°C gave a precipitate that showed a pure β X-ray diffraction pattern. If the solution is immediately quenched by placing it in an ice bath from T_R to a T_C of 10°C the β form is also obtained. As shown in Table III in the range of molecular weights used, ie 0.24×10^5 to 4×10^5, no systematic change in the DSC endotherm temperature is found. The endotherm was found to be very sharp for low molecular weight samples.

4. GROWTH of β - Form

Crystals grown from amyl acetate using T_D of 75 to 135°C and T_C in the region of -10 to 0°C exhibit strong endotherms in the region of 36 - 56°C (see Table V) and a very small endotherm for the α form at 63°C as shown in Fig.10. Heating to a T_D of 135°C, much above the melting point of the polymer, was done to destroy preexisting nuclei. The d spacings obtained from X-ray diffraction patterns are characteristic of the β structure and are given in Table VI. The wide range of endotherm values for the β form is

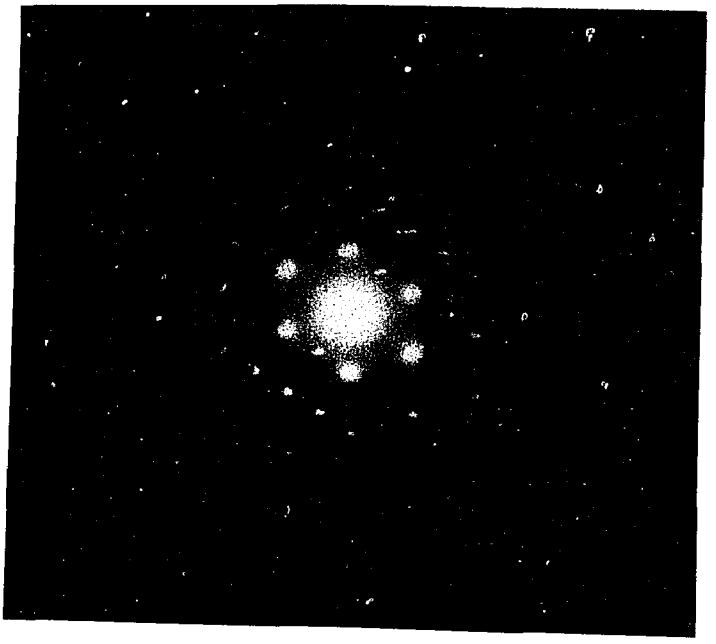

Fig. 9 Selected area diffraction pattern of a single crystal of the β form of trans 1,4 polyisoprene, grown from dilute amyl acetate solution. $\bar{M}_n = 2.9 \times 10^5$, $T_R = 50°C$ and $T_C = 20°C$

Table V

Density and DSC Endotherms of β TPI Crystals Grown from Dilute Amyl Acetate.

$\bar{M}_n$	$\bar{M}_w / \bar{M}_n$	T_D (°C)	T_C (°C)	Density g cm^{-3}	DSC Endotherm (°C)
$3.8x10^5$	1.5	115	-10	.969	36,44,53,61 (5:7 : 6: 1)*
$2.9x10^5$	1.4	135	0	-	48,54,61 (6: 6: 1)*
		100	0	.969	46,52 (2 :1)*
		100	0	.975	46,53,61 (6: 4: 1)*
$2.8x10^5$	1.4	100	0	.971	47,54,61 (3 : 5:1)*
$2.3x10^5$	1.3	130	0	.968	55,62 (8:1)*
		78	0	.967	47,55,61 (2: 7: 1)*
$1.1x10^5$	1.4	80	0	-	46,55,62 (2: 8: 1)*
$0.35x10^5$	4.84	100	0	.960	48,52 (1:1)*
		100	0	.971	57

* Ratio of endotherms interms of heights of the peak.

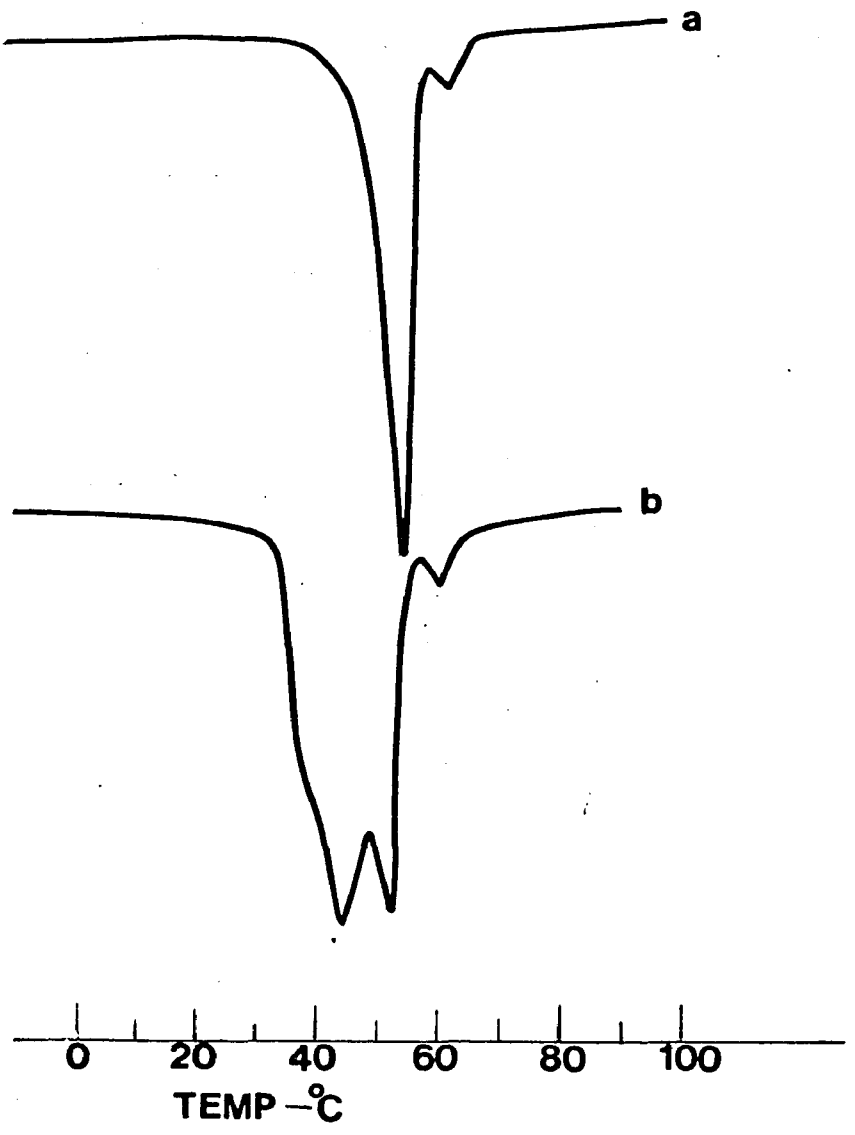

fig.10 DSC ENDOTHERMS OF β TRANS 1,4 POLYISOPRENE CRYSTALS GROWN FROM DILUTE AMYL ACETATE SOLUTION. $\bar{M}_n = 2.9 \times 10^5$ (a) $T_D = 80°C$ and $T_C = 0°C$ (b) $T_D = 80°C$ and $T_C = -10°C$.

Table VI

Comparison of Observed d-Spacings with Literature[56] Values for β Form

d-Observed (Å)		d-Literature (Å)
4.94	vs	4.73
4.13	vs	3.92
2.98	mw	2.98
2.79	mw	2.78
2.38	m	2.38
1.97	mw	1.97
1.93	m	1.77

w - weak

m - medium

s - strong

vs- very strong

apparently due to the continued presence of solvent after the drying process. This would lead to an annealing of the β form crystals when they are heated to room temperature prior to measurement. Multiple melting peaks are generally attributed to recrystallization processes occuring at a rate comparable to or greater than the heating rates normally used in differential thermal analysis.

5. MORPHOLOGY

Crystallization at 25 - 36°C of TPI with $\bar{M}_n$ of 2.5×10^5 from a T_R of 40°C gave small elongated hexagonal shaped crystals, a representative sample of this being given in Fig.11. Crystallization at 20°C as well as at 10°C with cooling from 40°C gave overgrown ellipsoidal shaped crystals as shown in Figures 12 and 13, while crystallization at 20°C with cooling from 50°C led to rectangular shaped crystals (see Fig.14). When low molecular weight fraction of Gutta Percha $\bar{M}_n$ of 1.92×10^4 was crystallized at 20°C and 30°C (T_R 40°C) overgrown hexagonal shaped crystals with sharp regular edges were formed as shown in Figures 15 and 16. The crystal size is approximately uniform since the crystals start to grow simultaneously from nuclei already present and each individual crystal is approximately representative

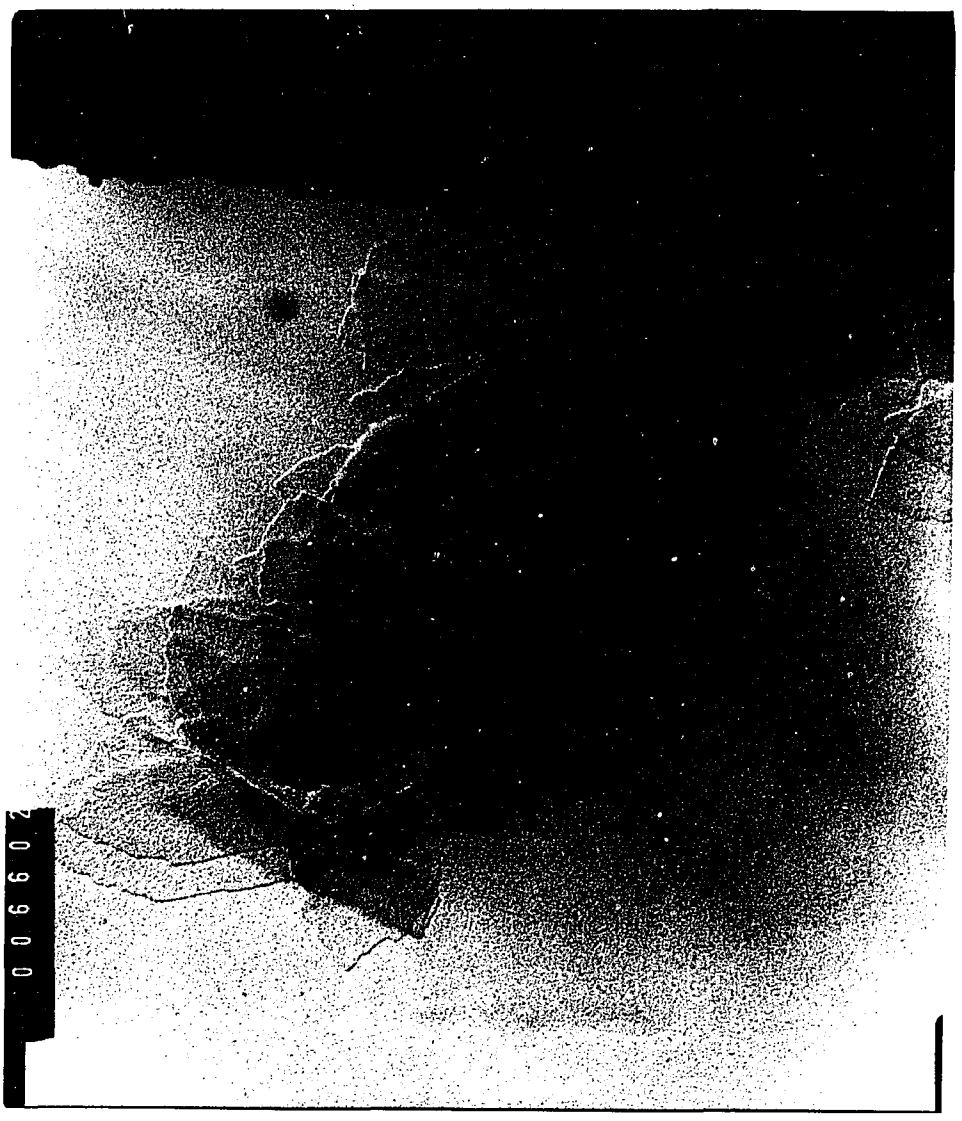

Fig. 11 Electron micrograph of trans 1,4 polyisoprene single crystal grown from dilute amyl acetate solution.

$\bar{M}_n = 2.9 \times 10^5$, $T_R = 40°C$ and $T_C = 30°C$

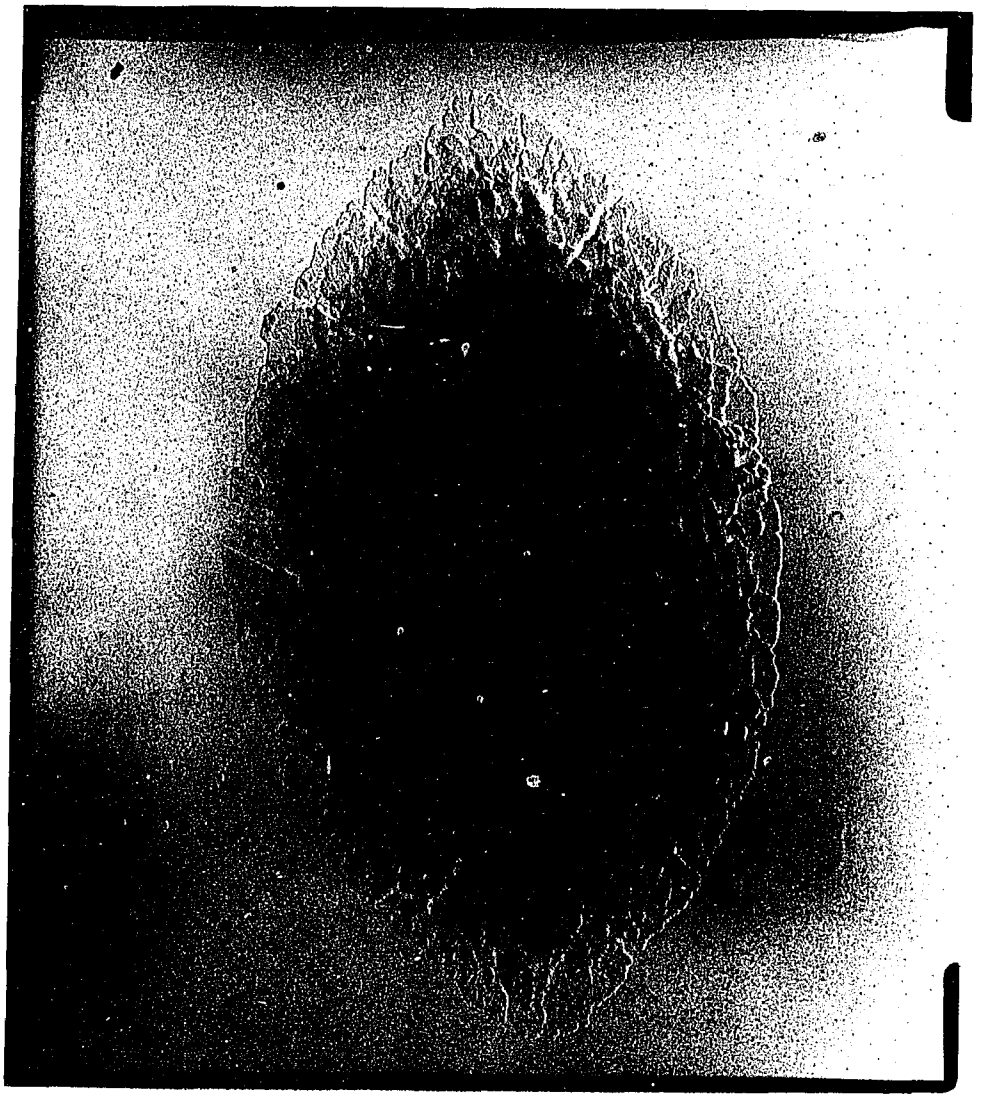

Fig. 12 Electron micrograph of trans 1,4 polyisoprene, single crystal grown from dilute amyl acetate solution.
$\bar{M}_n = 2.9 \times 10^5$, $T_R = 40°C$ and $T_C = 20°C$

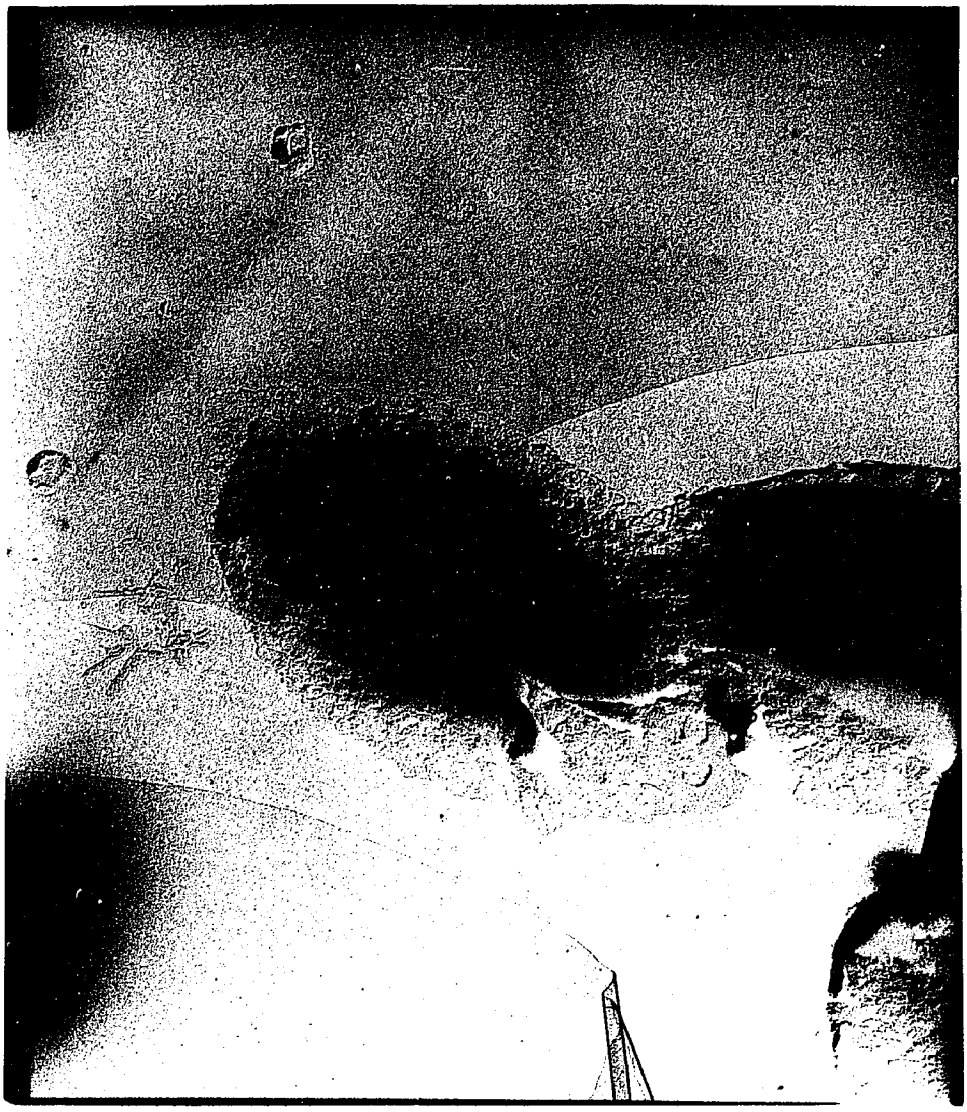

Fig. 13 Electron micrograph of trans 1,4 polyisoprene single crystal grown from dilute amyl acetate solution.
$\bar{M}_n = 2.9 \times 10^5$, $T_R = 40°C$ and $T_C = 10°C$

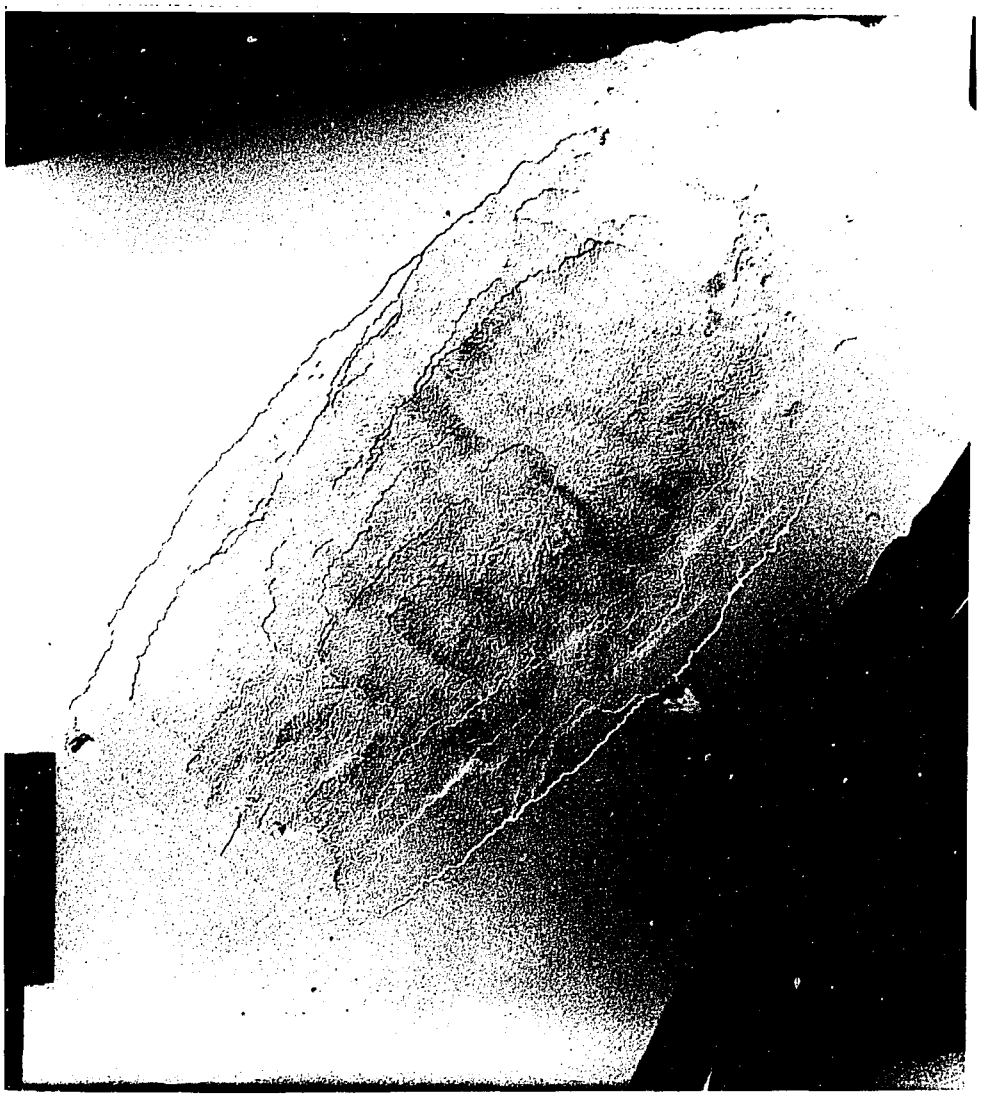

Fig. 14 Electron micrograph of trans 1,4 polyisoprene single crystal grown from dilute amyl acetate solution.
$\bar{M}_n = 2.9 \times 10^5$, $T_R = 50°C$ and $T_C = 20°C$.

Fig. 15 Electron micrograph of trans 1,4 polyisoprene single crystal grown from dilute amyl acetate solution.

$\bar{M}_n = 1.9 \times 10^4$, $T_R = 40°C$ and $T_C = 20°C$

Fig. 16 Electron micrograph of trans 1,4 polyisoprene single crystal grown from dilute amyl acetate solution.

$\bar{M}_n = 2.6 \times 10^4$, $T_R = 40^\circ C$ and $T_C = 30^\circ C$

of the preparation as a whole. When viewed under the optical microscope in suspension, the ellipsoidal shaped crystals were curved or of crescentlike shape. Therefore due to drying on a flat substrate these crystals were collapsed and formed ridges. The 0°C grown β crystals were difficult to observe under the electron microscope due to aggregation.

6. DENSITY MEASUREMENTS of DILUTE SOLUTION CRYSTALLIZED TPI.

The densities obtained for mats of α TPI crystals grown at various crystallization temperatures, T_C, from 0.05% amyl acetate solution, are given in Table VII as a function of the number average molecular weight $\bar{M}_n$. The number of separate samples studied is indicated in parenthesis, if more than one was used; these numbers include samples prepared by cooling from different temperatures since no systematic change in the density with this temperature, T_R, was noted. The largest number of measurements were made on the samples crystallized at a T_C of 20°C. At a T_C of 20°C, no systematic change in the density occurs with molecular weight from 3.8×10^5 to 0.69×10^5. A small increase in density is observed for T_C = 20°C, when the molecular weight is decreased to 0.26×10^5. If all determinations at a particular T_C are averaged, the values found are those given in the last column of Table VII; the average deviation for each of these was within ± 0.003.

Table VII

Density (g cm^{-3}) of α TPI Crystals Grown from Dilute Amyl Acetate Solution (T_R=40°C)

T_C (°C)	$\bar{M}_n x10^5$=3.8	2.9	2.8	2.3	2.1	1.1	0.69	0.26	AVE
0*		0.969(2)							0.969
10	0.970	0.970(2)	0.968(2)			0.963			0.969
20	0.974(5)	0.975(5)	0.970(2)	0.972(2)	0.973	0.974	0.973	0.978(2)	0.974
25	0.975	0.976(3)	0.975						0.976
30	0.982	0.978(4)	0.972(2)		0.970		0.976	0.981	0.977
32	0.980	0.978(4)	0.973(2)						0.977
34		0.980(2)							0.980
36			0.978						0.978

* X-ray Diffraction Shows Predominantly α Form.

The average density value is found to increase with increasing T_c in the 10 to 34°C range.

The effect on the density of keeping trans - 1,4-polyisoprene crystals in contact with amyl acetate at the crystallization temperature, 20°C, for one and two months with frequent changes of the liquid was monitored for a sample with $\bar{M}_n$ of 2.9×10^5. Density values of 0.971, 0.976 and 0.977g cm^{-3} were obtained for freshly prepared crystals and for crystals in contact with amyl acetate for one month and for two months, respectively.

A total noncrystalline content, $1-W_c$, at each T_c used was obtained from the density values in Table VII and are given in Table XVII. The average deviation for this quantity is $\pm$ 0.02. A decrease in $1-W_c$ with increasing T_c is seen to occur.

The densities obtained for mats of β TPI crystals from 0.05% amyl acetate solution are given in Table V. If all the values are averaged, the density value obtained was 0.969g cm^{-3} with an average deviation of $\pm$ 0.003.

7. LAMELLAR THICKNESS MEASUREMENT

The lamellar thickness was determined by electron microscopy for α TPI crystals prepared at T_c's of 10, 20, 25 and 30°C with a $\bar{M}_n$ of 2.9×10^5 (T_R = 40°C). The individual values obtained in different

fields for two sets of crystal preparations are given in Table VIII. The mean values are given in the last column; the average deviations for these measurements is ± 15Å. These measurements were calibrated using a PTBD sample of known lamellar thickness, obtained by LAXR measurements.

8. EFFECT of ANNEALING TPI SINGLE CRYSTALS on DENSITY and MELTING ENDOTHERM.

The results of annealing the β TPI crystals in the presence of acetone in deoxygenated sealed tubes are given in Table IX. As shown, the DSC endotherm values for annealing temperatures above 40°C have increased considerably, due to conversion to the α form; the density either remained constant or decreased. The n-butyl acetate annealed β TPI, showed an increase of 13°C in the DSC endotherm value and a small increase in density. This crystal mat appeared reprecipitated during the experiment. Acetone annealing of the α form at 40°C did not produce any change but after annealing at 55°C a major endotherm appeared at 75°C; this is 12°C higher than the starting one, however the density decreased to .959 from .973gm cm^{-3}. Table X contains the density and DSC endotherm values obtained for annealed α TPI crystals in sealed tubes filled with nitrogen. If the densities of samples with constant T_c's were averaged, (assuming no effect

Table VIII

The Lamellar Thickness of α TPI Crystals Grown from Dilute Amyl Acetate Solution, Obtained by Electron Microscopy. $\bar{M}_n = 2.9 \times 10^5$

T_R (°C)	T_C (°C)	Lamellar Thickness (Å)	Average (Å)
40	10	76,67,96,80,78,64	78
40	20	61,62,60,64,112,80	
		71,118,109,107,107,112,108	90
40	25	91,97,103,108,87	
		133,133,119,134,131,136	115
40	30	96,118,107,116	
		111,146,140,152,148,119	125

Table IX

Effect of Annealing in Acetone on the DSC Endotherm and Density for TPI Crystals Grown from Dilute Amyl Acetate Solution

$\bar{M}_n$	$\bar{M}_w / \bar{M}_n$	T_D (°C)	T_R (°C)	T_C (°C)	Anneal Temp (°C)	DSC Endotherm (°C) Initial	Final	Density (g cm^{-3}) Initial	Final	Anneal Time-Days
0.35×10^5	4.8	100		0	55	48,52	60,74	.960	.956	3
		100		0	50	48,52		.960	.957	3
		100		0	45	48,52	67	.960	.957	3
		100		0	40	48,52	48,54	.960	.960	3
		100		0	45	48,52	62,75	.960	.969	3*
1.10×10^5	1.4	85		0	55		62,73		.960	2
2.90×10^5	1.4	120		0	40	48,53	58,64			2
		80	40	20	40	62	62			2
2.80×10^5	1.4	80	40	30	40	67	67			2
3.80×10^5	1.5	80	40	20	55		64,75		.959	2

* Solvent n-Butyl Acetate.

Table X

Density and DSC Endotherms of Annealed α TPI Crystals Grown from Dilute Amyl Acetate Solution

$\bar{M}_n$	T_R (°C)	T_C (°C)	Annealing Temp (°C)	Density (g cm^{-3}) Initial	Final	DSC Endotherm (°C) Initial	Final	Annealing Time-Days
2.9×10^5	40	20	40	.971	.977	62	62	10
			49		.976			10
			49	.976	.973			10
	50	20	55	.979	.973	63	63	10
	40	25	42	.980	.982	64	64	10
			50	.980	.976	64	64	10
			50	.972	.984	64	64	10
	40	30	40	.978	.983	67	67	10
		32	45	.975	.991			10
3.8×10^5	40	30	50	.982	.989			10

due to annealing temperature) a small increase in density is observed, with no change in the endotherm value. The electron micrograph of an annealed crystal which is given in Fig.17 shows some changes along the edges due to thickening.

9. EPOXIDATION of CRYSTALS in SUSPENSION

In order to establish the use of ^1H NMR to quantitatively assay the fraction of double bonds epoxidized in TPI lamellas, results for synthetic TPI and for Balata epoxidized in $CHCl_3$ solution were obtained as given in Table XI.

Table XI Relative composition of Peroxidation Reaction Mixtures and the % Epoxidized Obtained from ^1H NMR Analysis for TPI Epoxidized in $CHCl_3$ Solution at 20°C.

Sample	Wt. of TPI (g)	Wt. of MCPBA(g)	Mole Ratio MCPBA / DB	% DB Reacted CH	CH_3
Sys TPI	.344	.224	.26	25	27
	.386	.275	.28	28	27
Balata	.706	.592	.33	33	34
	.465	.297	.25	25	25

The fraction of double bonds reacted as assessed from the CH and the CH_3 NMR shifts are given in the last two columns,

Fig. 17 Single crystal of α-TPI annealed at 50°C for 22 Hours on a carbon film.
$\bar{M}_n = 2.9 \times 10^5$ and $T_C = 20°C$

of this table. These results are in close agreement with the expected values as given in column 4. Completely soluble products containing up to 50% epoxide content were obtained by this technique. A typical ^{1}H NMR spectrum of TPI and partially epoxidized TPI is given in Figures 18 and 19. In Fig.20, a spectrum of completely epoxidized squalene, used as a model compound is shown.

The ^{1}H NMR spectrums (Fig's 19 and 20) indicate that the reaction is a simple addition reaction uncomplicated by side reactions and alternative routes, such as ring opening, hydroperoxide formation, isomerization or degradation. Thus the non-radical reaction, as proposed by the following mechanism[77], in which trans double bond yields only trans oxirane rings is probably occurring.

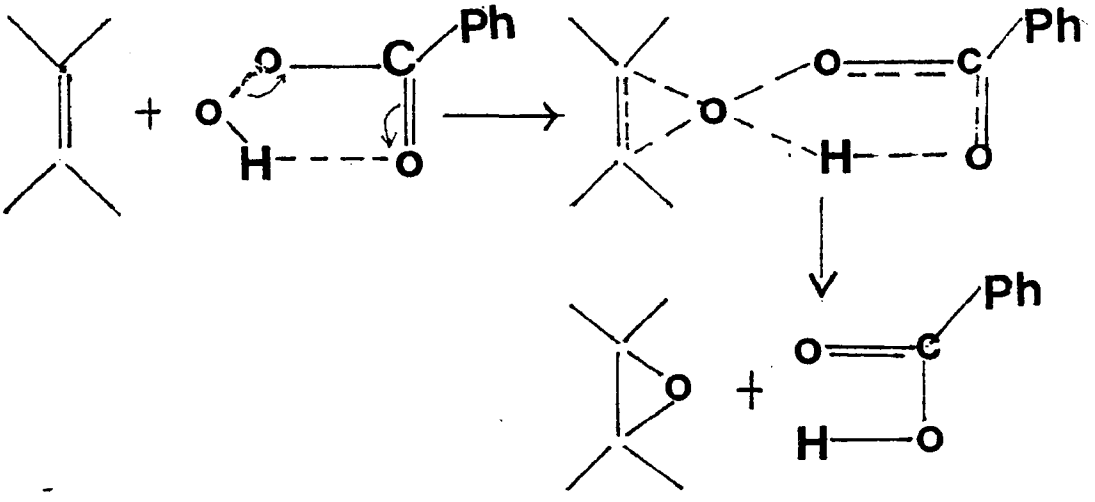

Epoxidation of α TPI crystals in suspension was carried out on five different preparations. The initial amount of reactants used in these experiments,

fig. 18 ^{1}H NMR SPECTRUM OF TPI IN $CDCl_3$ SOLUTION.

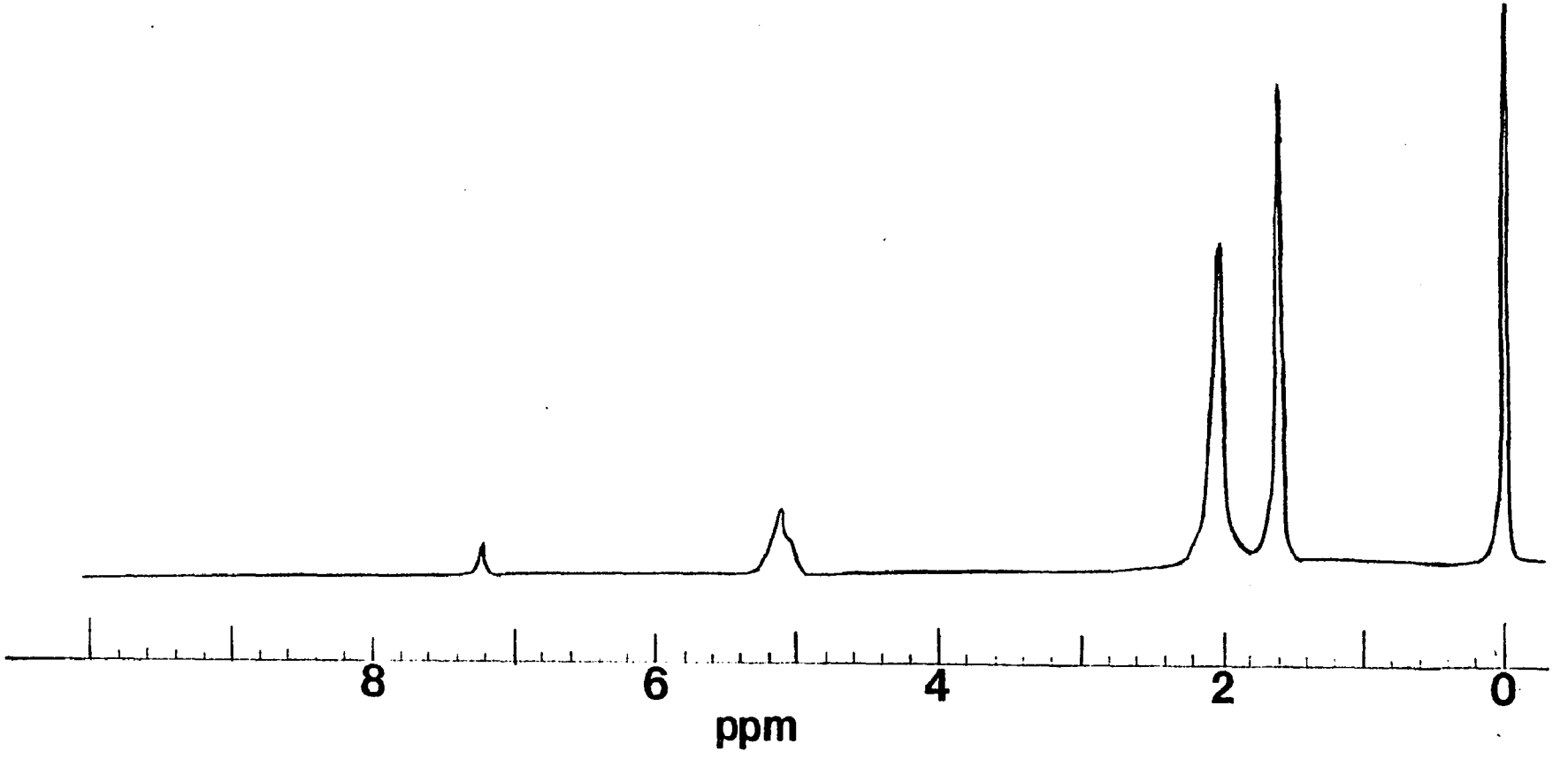

fig. 19 ^{1}H NMR SPECTRUM OF EPOXIDIZED TPI IN $CDCl_3$ SOLUTION.

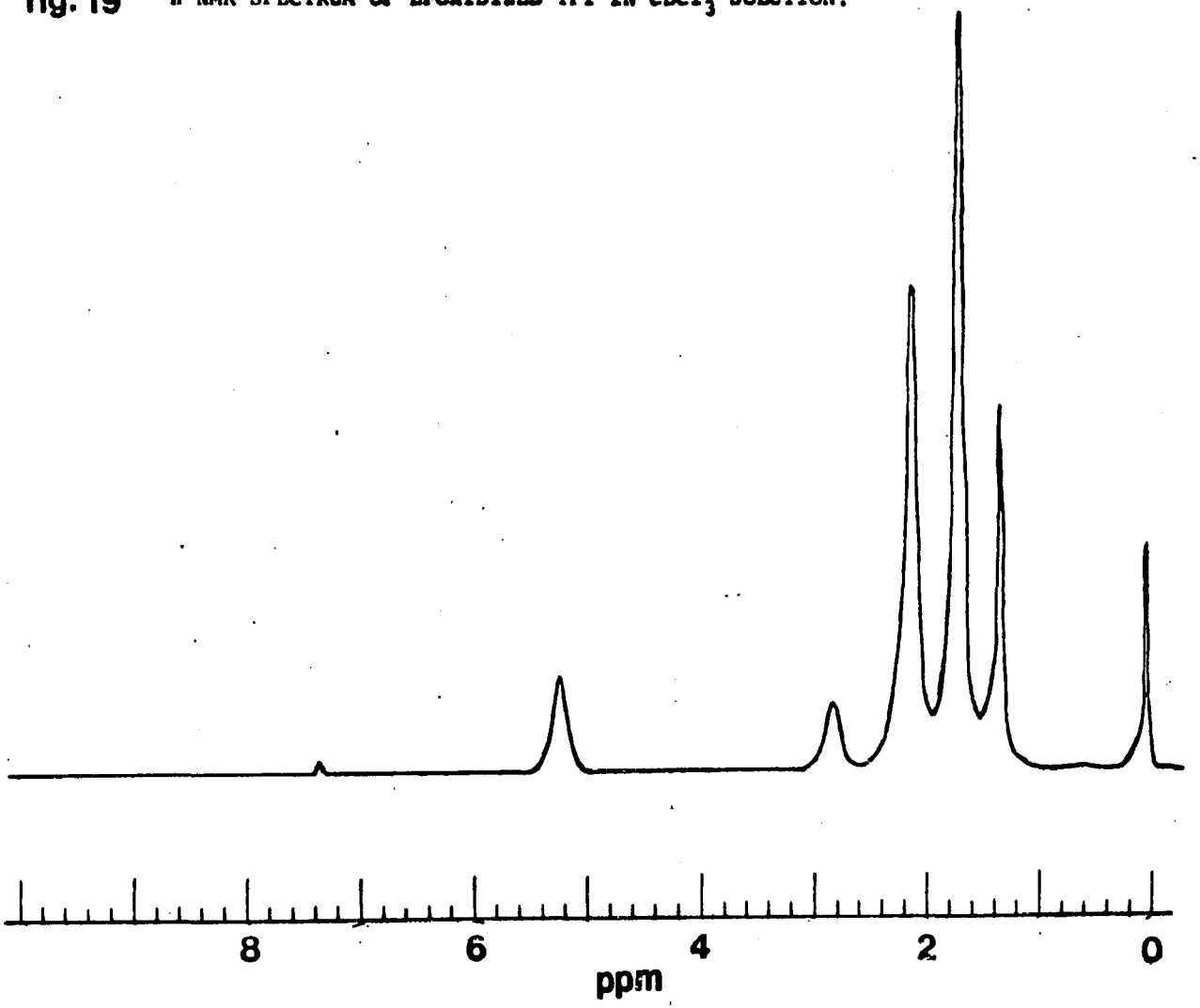

fig. 20 ^{1}H NMR SPECTRUM OF COMPLETELY EPOXIDIZED SQUALENE IN $CDCl_3$ SOLUTION.

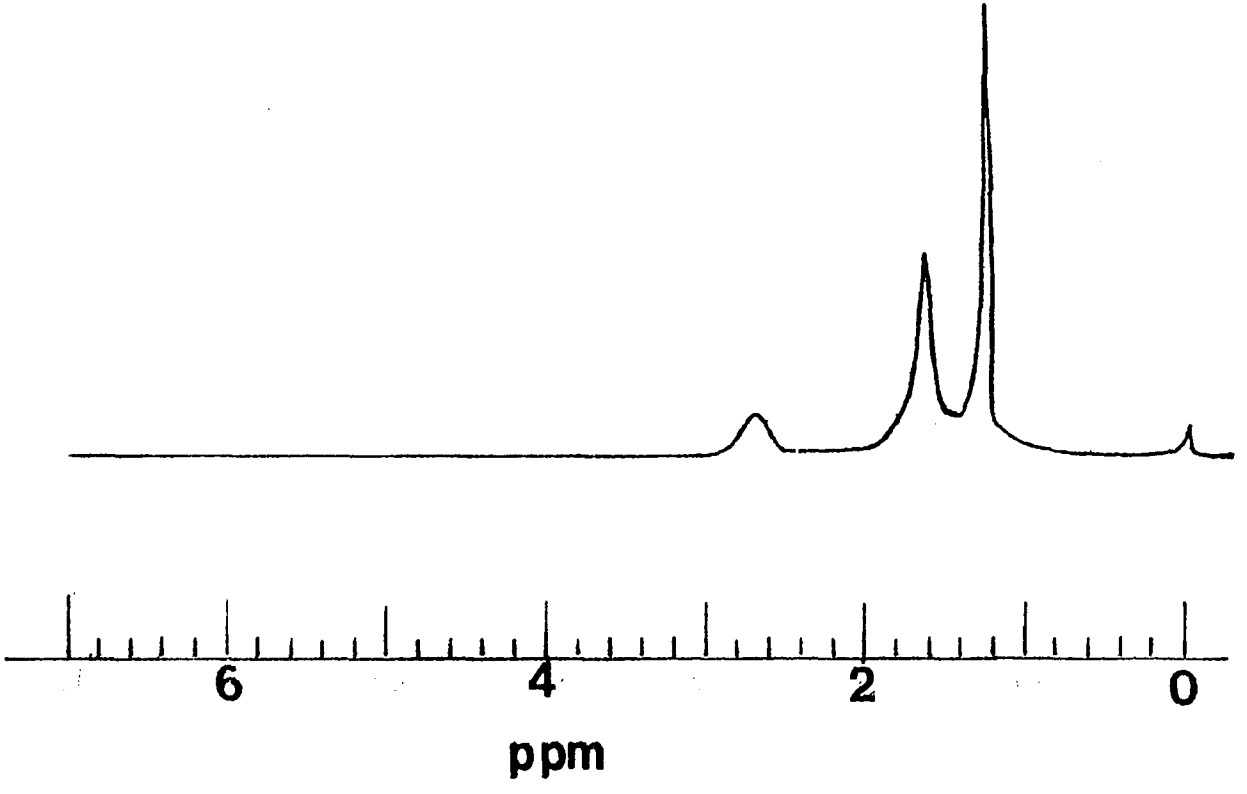

the epoxidation time and the amount reacted are given in Tables XII-XIV. The molar ratio of MCPBA to double bonds was calculated assuming complete precipitation of the polymer during crystallization. Therefore these values represent the minimum ratio; the actual ratio at the start of epoxidation will be higher especially for lower molecular weight samples. Further, on analyzing the extent of reaction it is clear that the amount of MCPBA initially present is in excess of that needed to react with the available double bonds. Duplicate determinations agreed within ±0.02.

The fraction of double bonds epoxidized at various times in amyl acetate at 0°C as given in Tables XII- XIV is plotted in Figures 21-25. It can be seen from these data that from 25-40% of the total number of double bonds present are epoxidized after two days under the conditions used. The reaction rate then diminishes, and at least for three of the five preparation studied, the amount epoxidized becomes constant after about six additional days. This is then taken as representative of the fraction of monomer units at the lamellar surfaces, F_S. With respect to the T_C = 30°C preparation (Fig.23) a constant value was not reached; therefore the fraction found after 28 days of reaction was used, thereby representing a lower limit. The limits of precision for F_S are the average deviations in the available data points; this is seen to

Table XII

Relative Composition of Peroxidation Reaction Mixtures and the % Epoxidized at 0°C in Amyl Acetate for α TPI Lamellas of $\bar{M}_n = 2.9 \times 10^5$ and $T_c = 20°C$.

Wt. of TPI Crystallized	$(MCPBA)_o$ g/100cm^3	Mole Ratio MCPBA / DB	Epoxidation Time-Days	% DB Reacted
0.08	0.156	.77	1	30
0.08	0.161	.80	2	35.5
0.08	0.158	.78	4	39.5
0.107	0.208	.77	2	29
0.107	0.208	.77	4	33
0.102	0.20	.77	8	40
0.103	0.20	.77	16	45
0.107	0.208	.77	8	39.5
0.107	0.208	.77	16	45.5
0.10	0.099*	.77	20	40
0.10	0.099*	.78	27	44.5
0.10	0.100*	.79	34	54
0.20	0.202*	.80	20	39
0.20	0.196*	.77	20	39

* An equal amount of MCPBA was added after 7 days.

Table XIII

Relative Composition of Peroxidation Reaction Mixtures and the % Epoxidized at 0°C in Amyl Acetate for α TPI Lamellas of (A) $\bar{M}_n = 2.9 \times 10^5$ and $T_c = 30°C$
(B) $\bar{M}_n = 2.1 \times 10^5$ and $T_c = 10°C$

	Wt. of TPI Crystallized	$(MCPBA)_o$ g/100cm^3	Mole Ratio MCPBA / DB	Epoxidation Time-Days	% DB Reacted
A.	.10	.199	.78	2	26
	.10	.208	.82	4	28
	.10	.201	.79	8	33
	.10	.203	.80	16	38
	.103	.203	.78	2	27.5
	.103	.211	.79	4	29
	.103	.205	.81	8	30
	.103	.201	.77	16	35
	.192	.178*	.73	28	38
	.196	.188*	.76	28	37
	.10	.083*	.66	16	37
B.	.12	.224	.74	2	37
	.12	.224	.74	4	44
	.12	.224	.74	8	58
	.12	.224	.74	16	58
	.106	.112*	.83	20	46
	.106	.110*	.81	27	53

*. An equal amount of MCPBA was added after 7 days.

Table XIV

Relative Composition of Peroxidation Reaction Mixtures and the % Epoxidized at 0°C in Amyl Acetate for α TPI Lamellas of (A) $\bar{M}_n = .69 \times 10^5$ and $T_c = 20°C$
(B) $\bar{M}_n = .26 \times 10^5$ and $T_c = 20°C$

	Wt. of TPI Crystallized	$(MCPBA)_o$ g/100cm^3	Mole Ratio MCPBA / DB	Epoxidation Time-Days	% DB Reacted
A.	.105	.208	.78	2	33.3
	.105	.208	.78	4	31.7
	.105	.208	.78	8	34.7
	.105	.208	.78	16	48.4
	.118	.224	.75	2	30.6
	.118	.224	.75	4	33.7
	.118	.224	.75	8	37.4
	.118	.224	.75	16	45
	.10	.192	.76	20	45.5
	.10	.192	.76	22	41
B.	.10	.195	.77	4	31.4
	.10	.195	.77	8	32.3
	.102	.20	.77	2	25
	.102	.202	.78	4	29
	.102	.198	.765	8	33.1
	.102	.194	.75	16	32.7

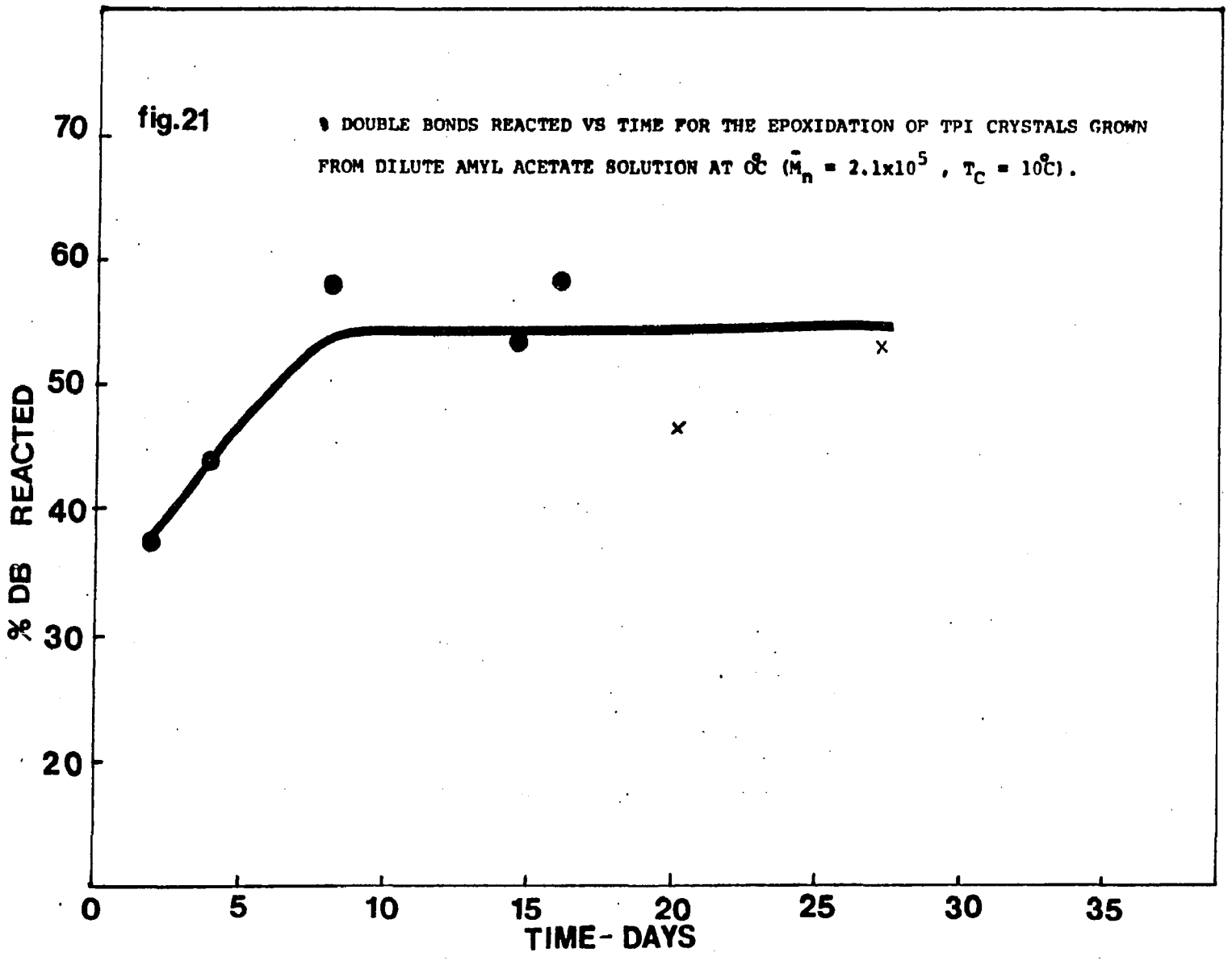

fig.21 % DOUBLE BONDS REACTED VS TIME FOR THE EPOXIDATION OF TPI CRYSTALS GROWN FROM DILUTE AMYL ACETATE SOLUTION AT 0°C ($\bar{M}_n = 2.1 \times 10^5$, $T_c = 10°C$).

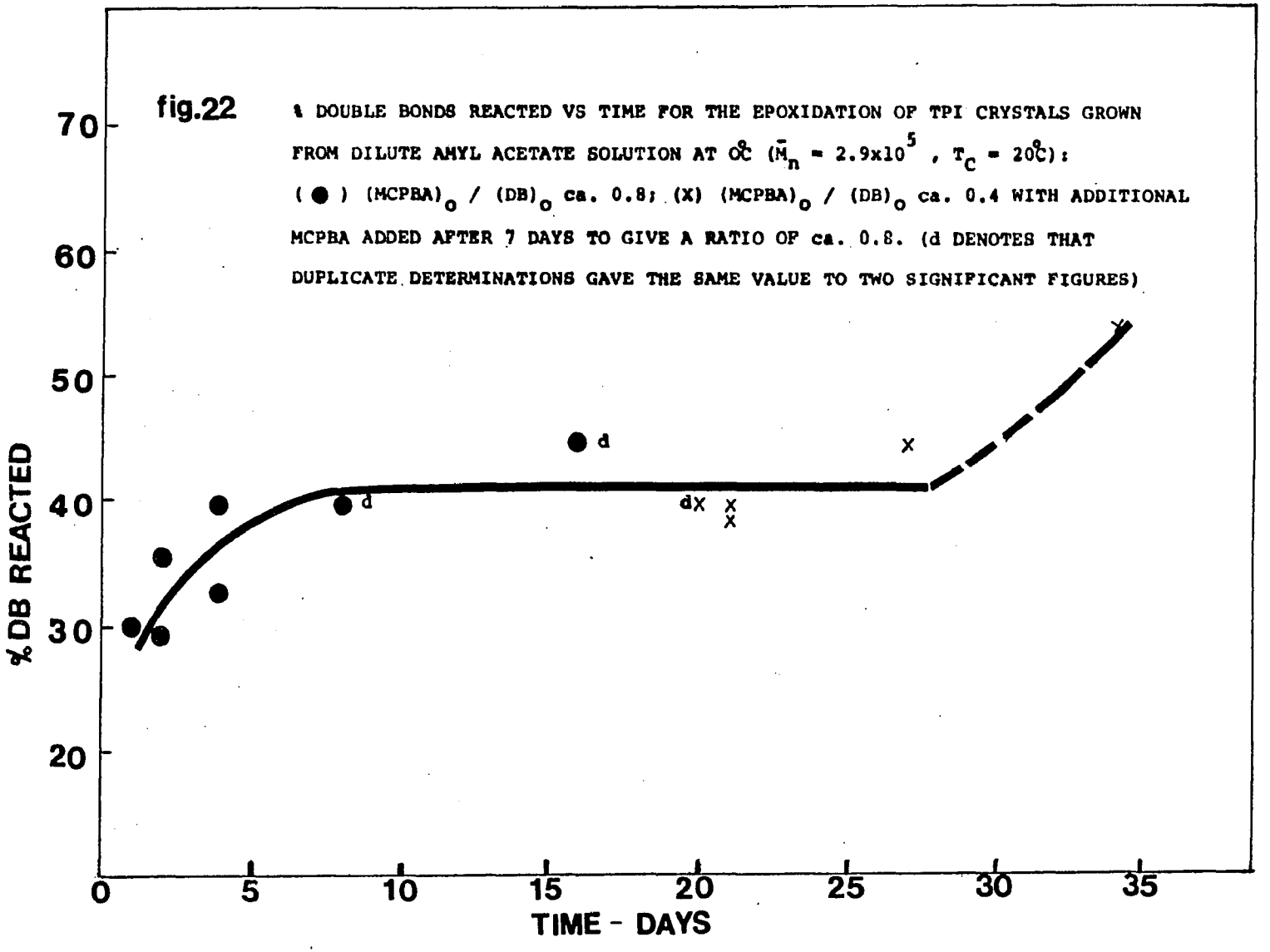
fig.22
% DOUBLE BONDS REACTED VS TIME FOR THE EPOXIDATION OF TPI CRYSTALS GROWN FROM DILUTE AMYL ACETATE SOLUTION AT 0°C ($\bar{M}_n$ = 2.9x10^5 , T_c = 20°C): (●) $(MCPBA)_o$ / $(DB)_o$ ca. 0.8; (X) $(MCPBA)_o$ / $(DB)_o$ ca. 0.4 WITH ADDITIONAL MCPBA ADDED AFTER 7 DAYS TO GIVE A RATIO OF ca. 0.8. (d DENOTES THAT DUPLICATE DETERMINATIONS GAVE THE SAME VALUE TO TWO SIGNIFICANT FIGURES)
% DB REACTED
70
60
50
40
30
20
0
5
10
15
20
25
30
35
TIME - DAYS
d
d
dX
X
X
X

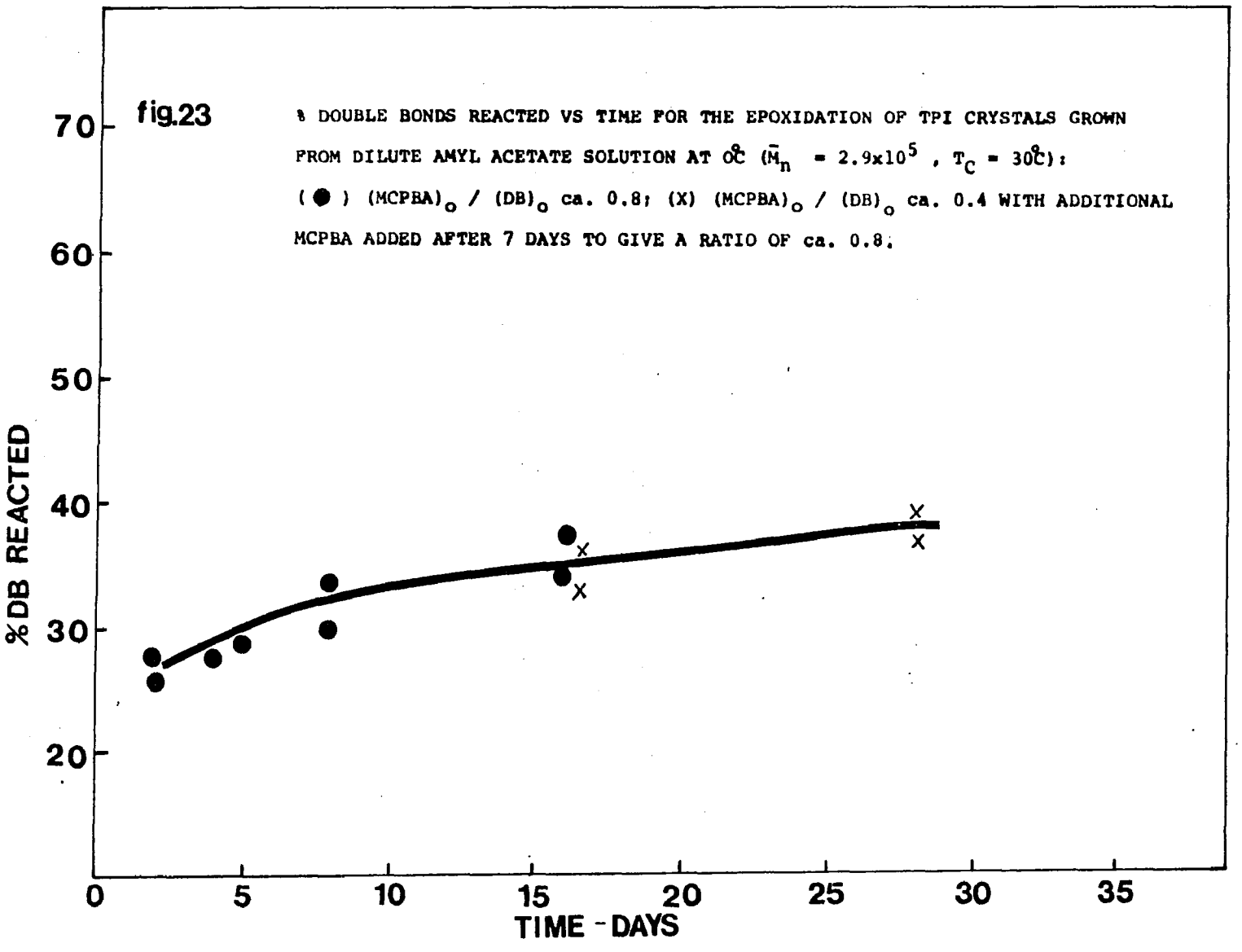
fig.23
% DOUBLE BONDS REACTED VS TIME FOR THE EPOXIDATION OF TPI CRYSTALS GROWN FROM DILUTE AMYL ACETATE SOLUTION AT 0°C ($\bar{M}_n$ = 2.9x10^5 , T_c = 30°C): (●) $(MCPBA)_o$ / $(DB)_o$ ca. 0.8; (X) $(MCPBA)_o$ / $(DB)_o$ ca. 0.4 WITH ADDITIONAL MCPBA ADDED AFTER 7 DAYS TO GIVE A RATIO OF ca. 0.8.
% DB REACTED
70
60
50
40
30
20
0
5
10
15
20
25
30
35
TIME - DAYS

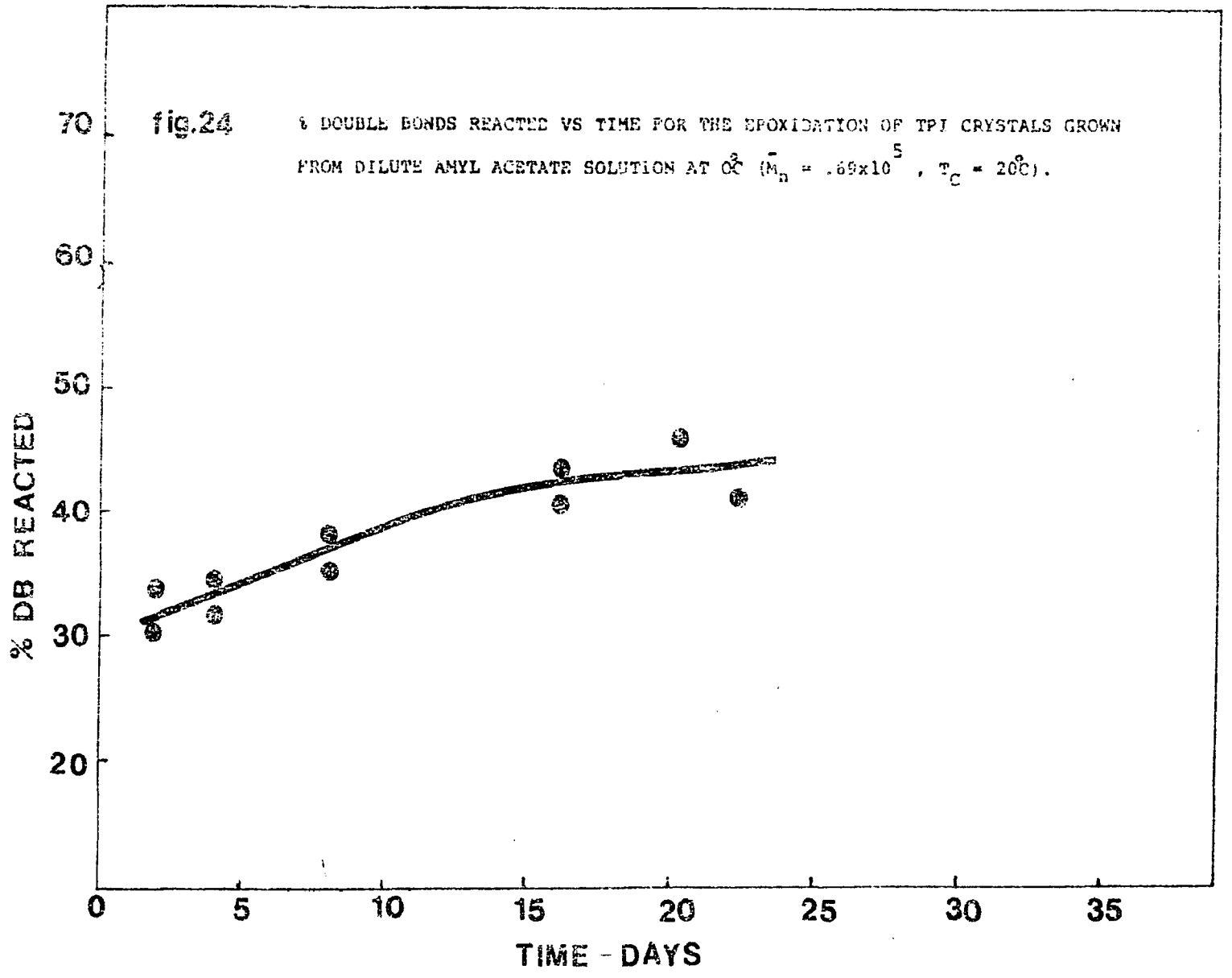

fig.24 % DOUBLE BONDS REACTED VS TIME FOR THE EPOXIDATION OF TPI CRYSTALS GROWN FROM DILUTE AMYL ACETATE SOLUTION AT 0°C ($\bar{M}_n = .69 \times 10^5$, $T_c = 20°C$).

fig.25 % DOUBLE BONDS REACTED VS TIME FOR THE EPOXIDATION OF TPI CRYSTALS GROWN FROM DILUTE AMYL ACETATE SOLUTION AT 0°C ($\bar{M}_n = 2.6 \times 10^4$, $T_c = 20°C$).

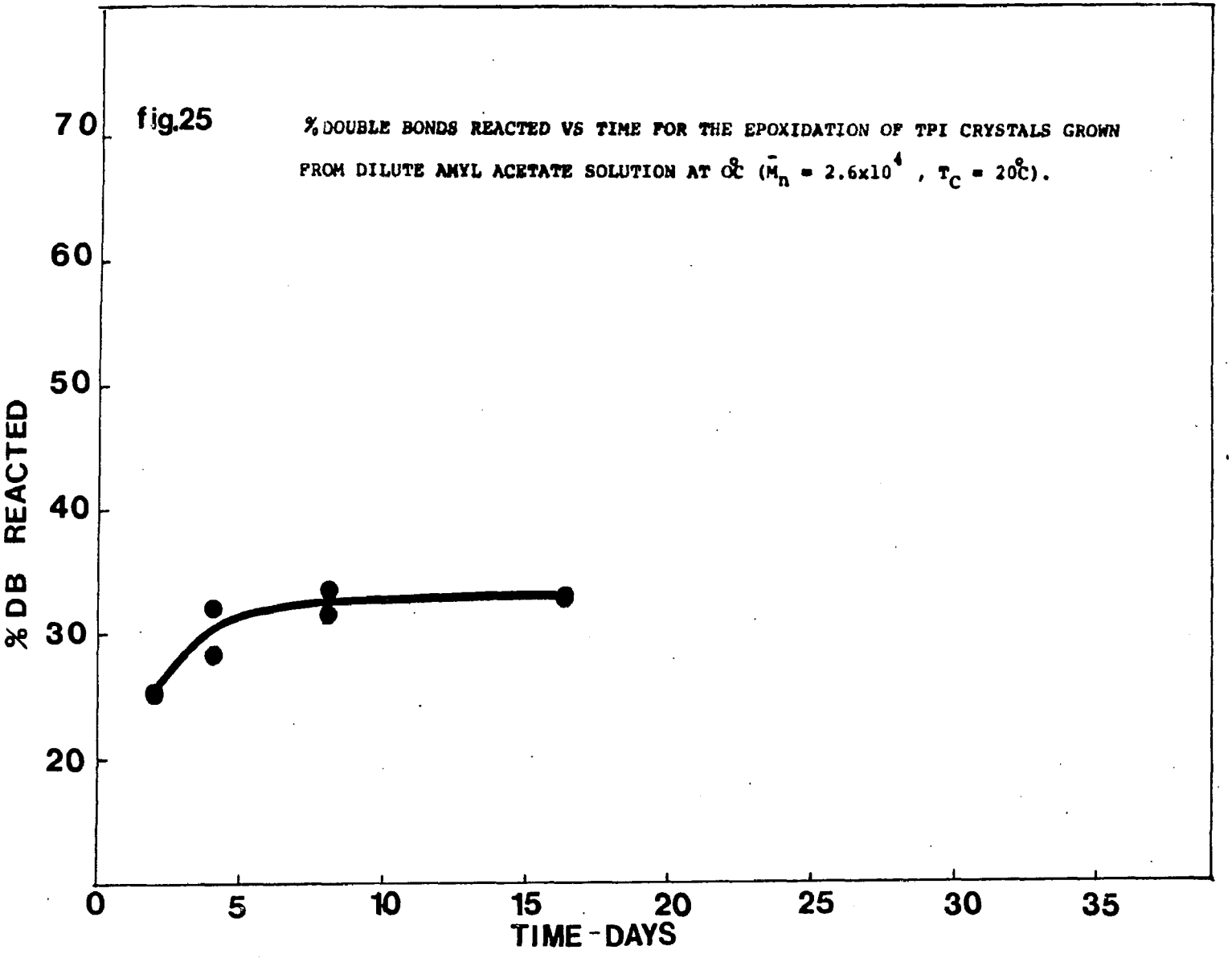

to be largest for the samples prepared at the lowest crystallization temperature (10°C).

Using $(MCPBA)_o$ = .1gm per $100cm^3$ with MCPBA / DB ca 0.4 the amount of material epoxidized levelled off with the epoxidation value of 28-30% in 5-8 days (see Table XV). On further addition of .1gm of MCPBA per $100cm^3$ a further reaction was observed when analyzed after 3-4 weeks. As shown in Figures 21-25 (the points with cross) these results fit with the curve obtained for samples with MCPBA / DB ca 0.8 and $(MCPBA)_o$ ca 0.2gm per $100cm^3$.

Table XV Relative Composition of Peroxidation Reaction Mixtures and the % Epoxidized at 0°C in Amyl Acetate for α TPI Lamellas of

(A) $\bar{M}_n = 1.1x10^5$ $\bar{M}_w / \bar{M}_n = 1.4$ and $T_C = 20°C$

(B) $\bar{M}_n = .345x10^5$ $\bar{M}_w / \bar{M}_n = 4.84$ and $T_C = 20°C$.

	Wt. of TPI Crystallized	$(MCPBA)_o$ g/$100cm^3$	Mole Ratio MCPBA / DB	Epoxidation Time-Hrs	% DB Reacted
A.	.122	.126	.41	120	28.5
	.110	.125	.45	140	28.3
	.110	.125	.45	164	28.5
B.	.107	.104	.38	114	27
	.109	.104	.38	140	27.5

A few epoxidation experiments were performed using $(MCPBA)_o$ other than 0.2g per $100cm^3$ with $(MCPBA)_o$ / DB = 0.80. Using the preparation with $\bar{M}_n$ of $2.1x10^5$ the following results were obtained.

T_c (°C)	$(MCPBA)_o$ g per $100cm^3$	Time Days	Fraction Epoxidized
20	.1	10	.43
20	.4	8	.47
20	1.0	8	.61
30	1.0	8	.49

Comparison of these results with those in Figures 22 and 23 shows that at least at $(MCPBA)_o$ = 1.0g per $100cm^3$ the epoxidation amount is about 50% higher than those obtained at 0.1 and 0.2g per $100cm^3$. Electron microscopy was carried out on epoxidized trans 1,4-polyisoprene lamellas recovered after two to thirty-five days reaction. The amount of damage to the crystals was assessed in a qualitative way as light (L), medium (M), heavy (H) and very heavy (VH) as given in Table XVI. Here crystals with lighter damage exhibited mainly fewer small holes. As the damage increased the number of holes increased, further the heavily damaged crystals became smaller due to erosion along the sides.

Table XVI

Electron Microscope Observations of Epoxidized TPI Crystals

$\bar{M}_n$	T_c (°C)	Epoxidation Time-Days	$(MCPBA)_o$ g per 100 cm^3	Damage[a]
$2.6x10^4$	20	4	0.2	L
		8	0.2	L
		16	0.2	L
$6.9x10^4$	20	8	0.2	L
		16	0.2	M
$2.1x10^5$	10	16	0.2	H
	20	8	1.0	VH
	30	8	1.0	H
$2.9x10^5$	20	2	0.2	M-(H)
		4	0.2	M
		16	0.2	M
		21	0.2	M
		35	0.1b	VH
	30	8	0.2	L
		16	0.2	L
		27	0.2	L-M

a. L=light; M= moderate; H = heavy; VH = very heavy

b. An equal amount of MCPBA was added after 7 days.

The material removed from the crystals and completely epoxidized won't affect the calculation of the fraction of double bonds reacted, since it would have been removed during washing. However due to the exposed holes, a slightly higher amount of reacted double bonds will be given. Examples of these are shown in the electron micrographs given in Figures 26-33. It was found that crystal damage increases with increasing $\bar{M}_n$, $(MCPBA)_o$ and reaction time and with decreasing T_c. The X-ray diffraction pattern of an epoxidized sample (T_c = 30°C, epoxidized for 28 days) indicate that the same crystal structure prevails as before the reaction, which suggests that the reaction of double bonds takes place mainly on the crystal surface.

The effect of keeping epoxidized crystals in contact with amyl acetate at 0°C to bring about desorption of any adsorbed noncrystalline material was studied using crystals from a preparation with $\bar{M}_n$ of 2.9×10^5 and T_c of 20°C that had been epoxidized for 21 days. The epoxidized crystals were washed and left suspended in amyl acetate while over the next 45 days the wash liquid was changed four times. Electron microscope examination of epoxidized crystals after suspension in amyl acetate for 30 days showed considerable loss of material from the edges (Fig.34) when compared with epoxidized crystals receiving the usual washing procedure (Fig.33). Not all of the crystals

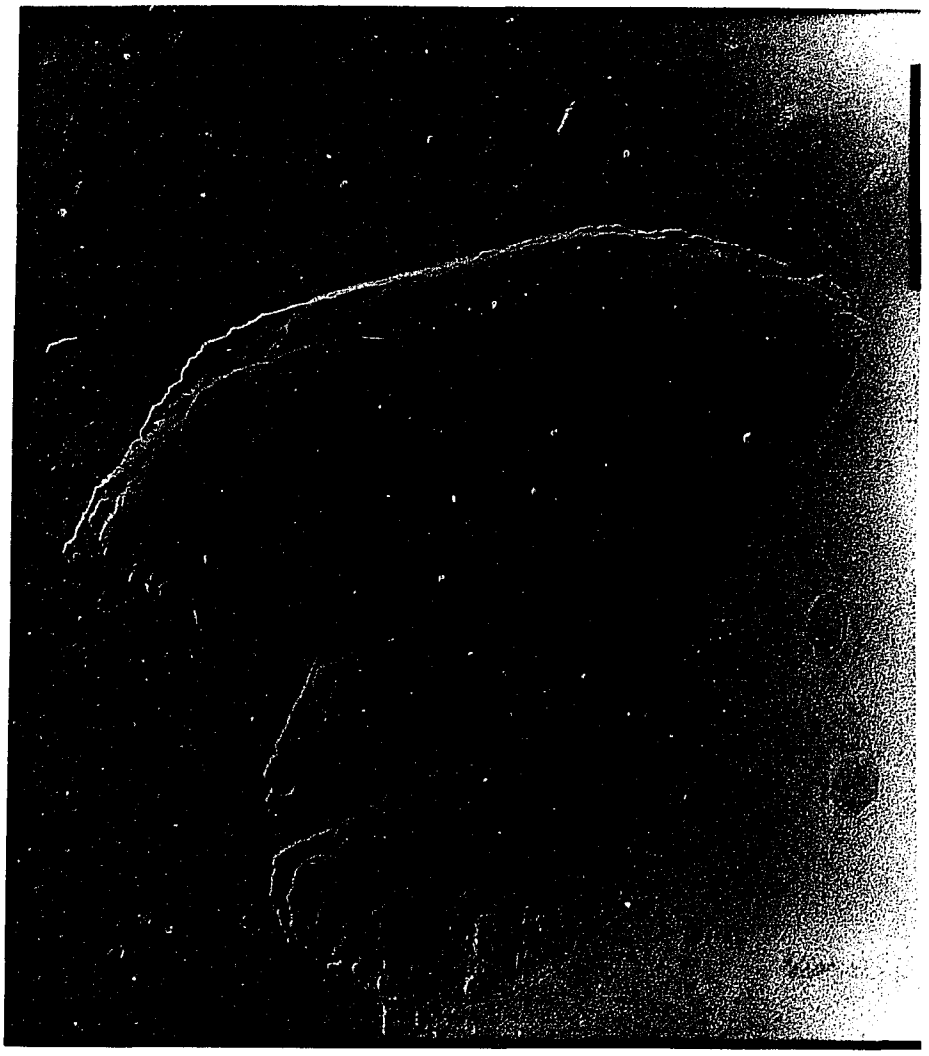

Fig. 26 Electron micrograph of epoxidized TPI crystals $\bar{M}_n = 2.6 \times 10^4$, $T_C = 20°C$ in amyl acetate at $0°C$ for 16 days.

Fig. 27 Electron micrograph of epoxidized TPI crystals ($\bar{M}_n = 6.9 \times 10^4$, $T_c = 20°C$) in amyl acetate at $0°C$ for 16 days.

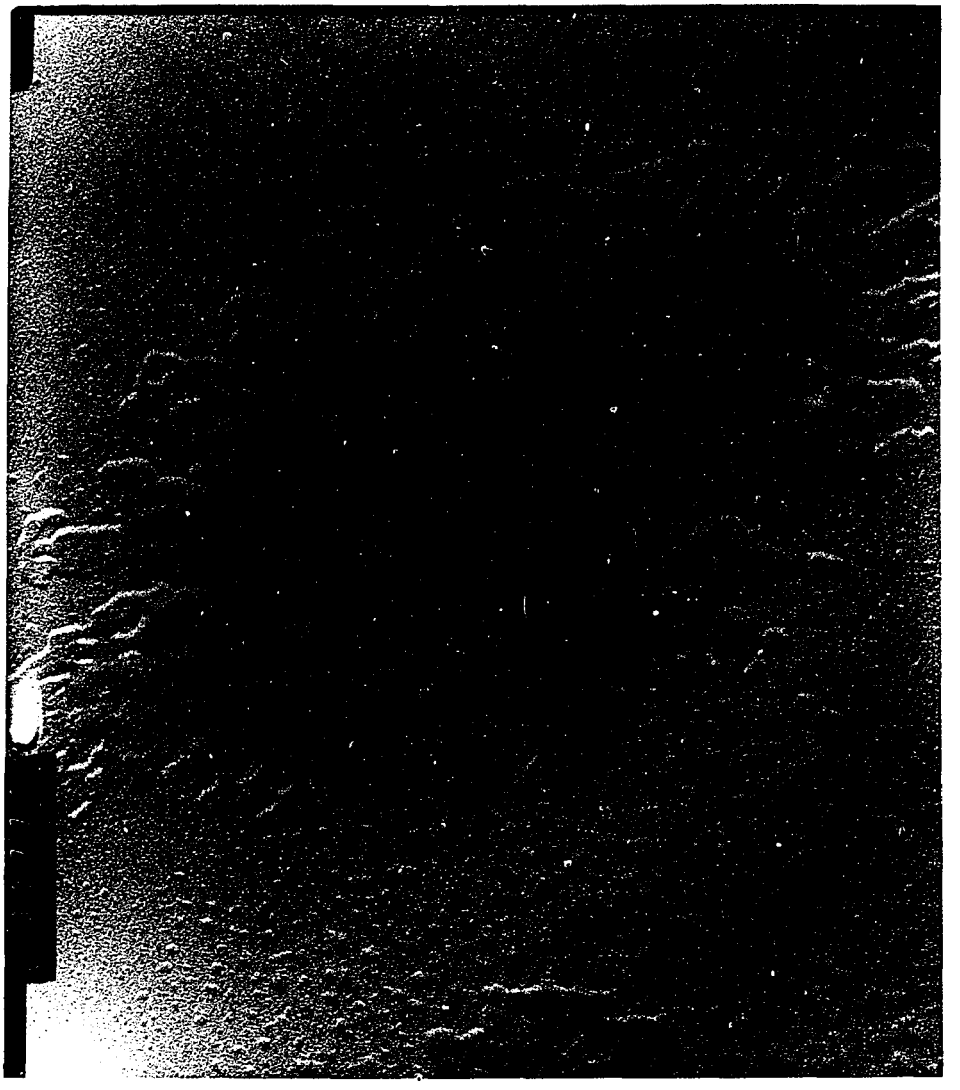

Fig. 28 Electron micrograph of epoxidized TPI crystals ($\bar{M}_n = 2.1 \times 10^5$, $T_C = 10°C$) in amyl acetate at 0°C for 16 days.

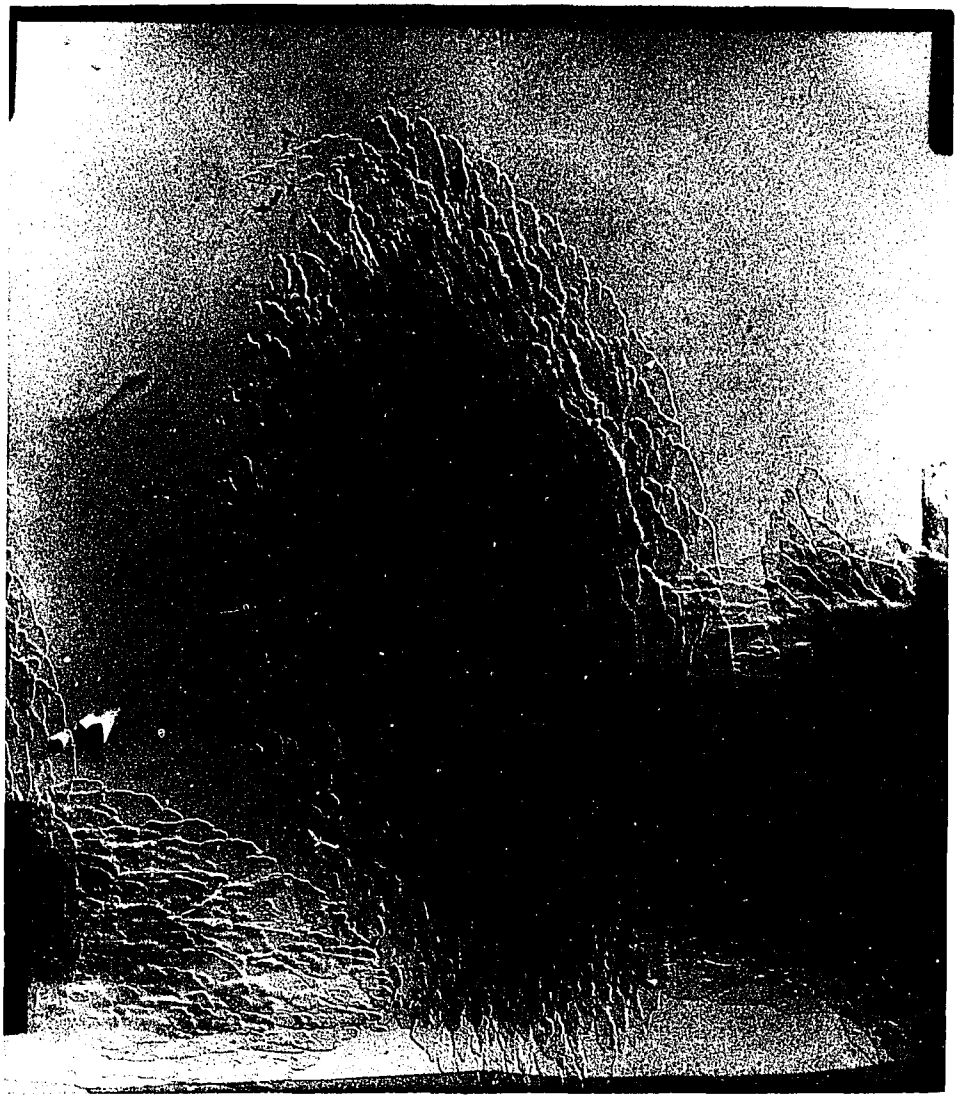

Fig. 29 Electron micrograph of epoxidized TPI crystal ($\bar{M}_n = 2.9 \times 10^5$, $T_c = 30^\circ C$) in amyl acetate at $0^\circ C$ for 16 days.

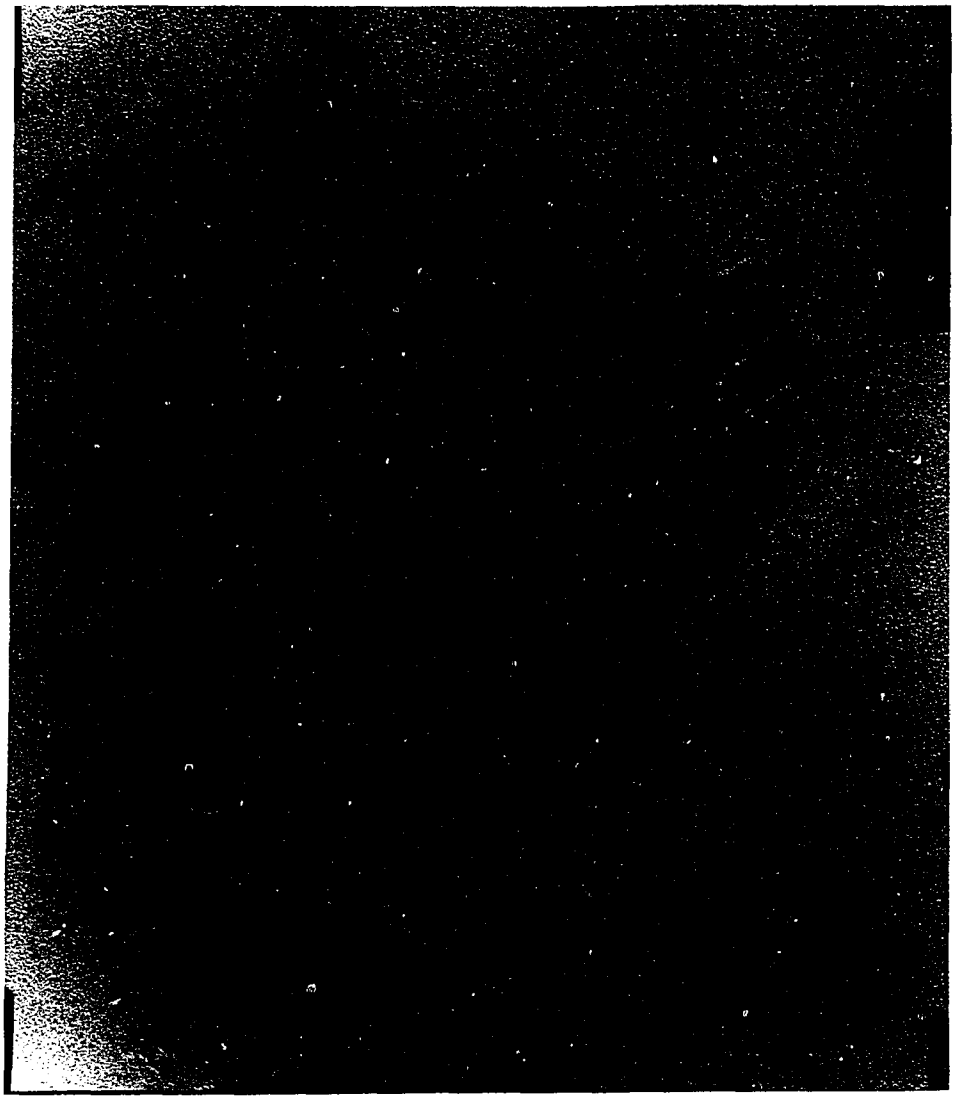

Fig. 30 Electron micrograph of epoxidized TPI crystal ($\bar{M}_n = 2.9 \times 10^5$, $T_c = 30°C$) in amyl acetate at $0°C$ for 27 days.

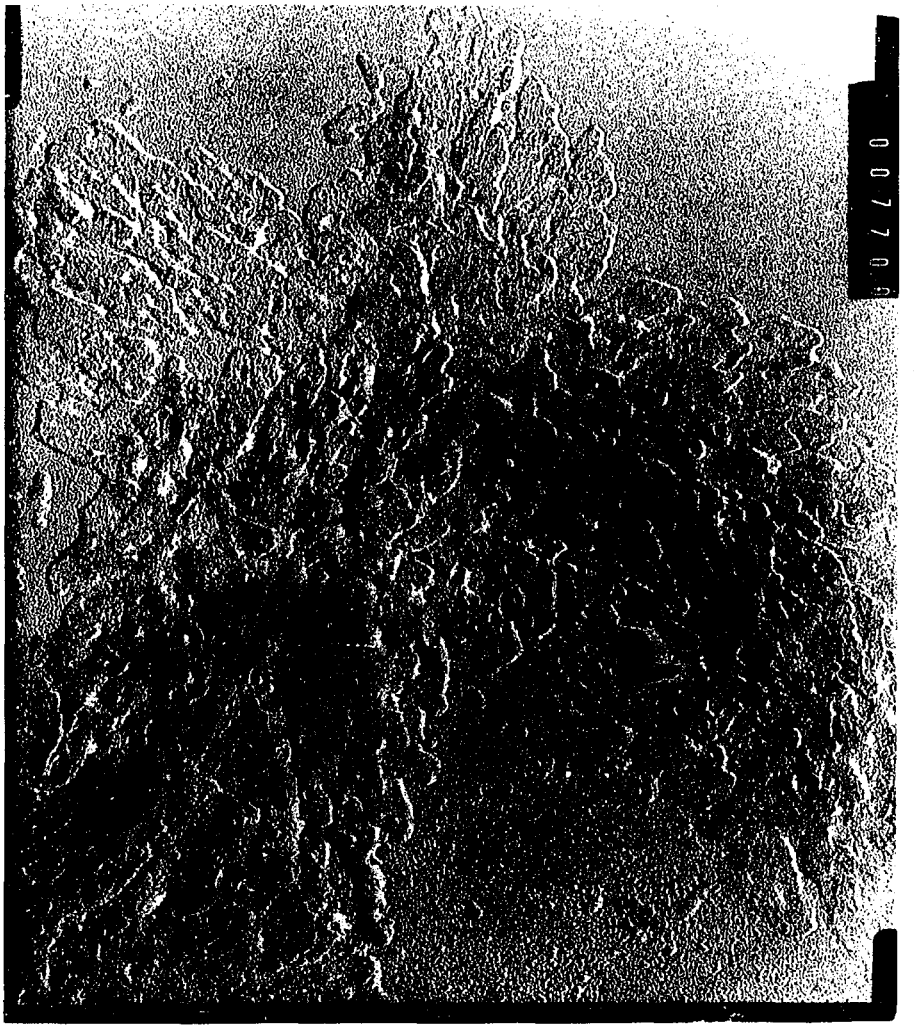

Fig 31 Electron micrograph of epoxidized TPI crystals ($\bar{M}_n = 2.1 \times 10^5$, $T_c = 20^\circ C$) in amyl acetate at $0^\circ C$ for 8 days, with MCPBA concentration of 1.0% (W/V).

Fig. 32 Electron micrograph of epoxidized TPI crystals ($\bar{M}_n = 2.9 \times 10^5$, $T_c = 20°C$) in amyl acetate at 0°C for 4 days.

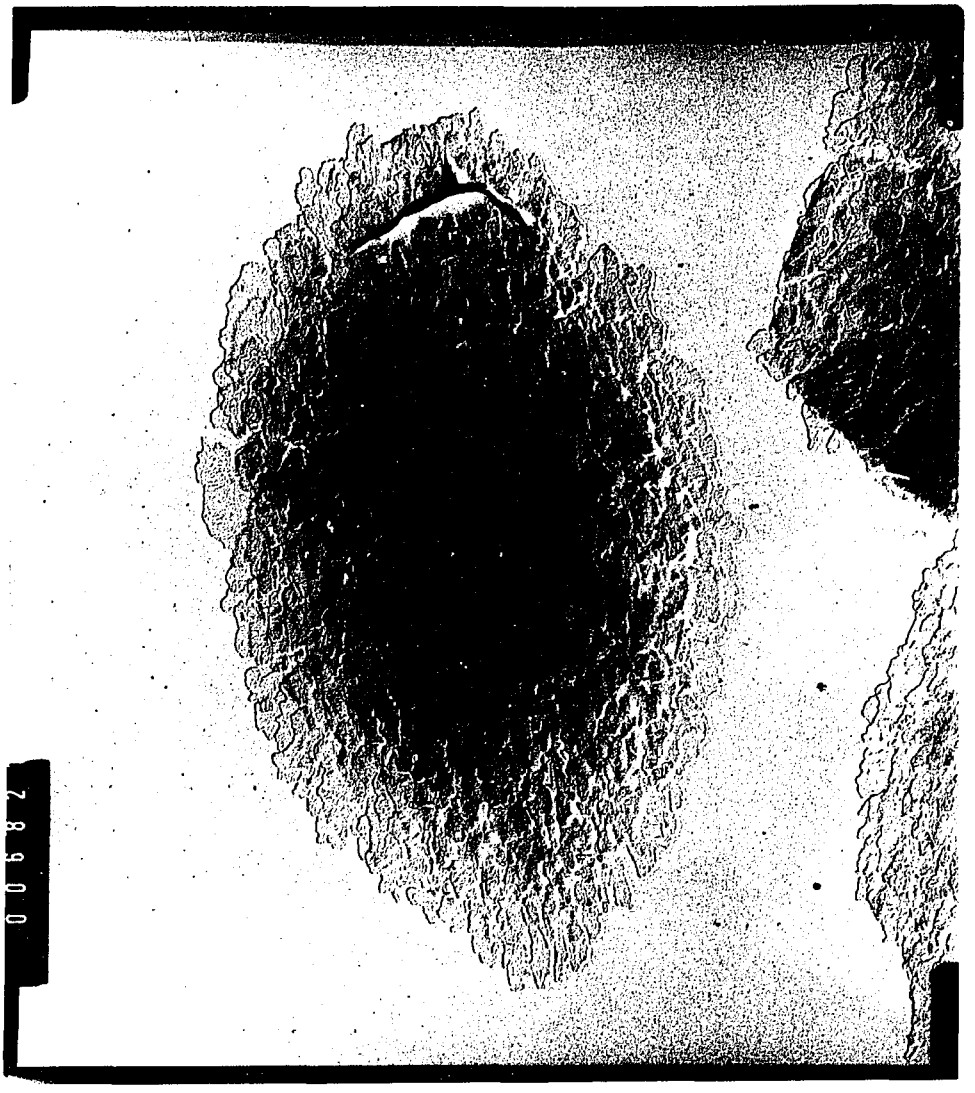

Fig. 33 Electron micrograph of epoxidized TPI crystals ($\bar{M}_n = 2.9 \times 10^5$, $T_C = 20°C$) in amyl acetate at 0°C for 21 days.

Fig. 34 Electron micrograph of epoxidized TPI crystal ($\bar{M}_n = 2.9 \times 10^5$, $T_c = 20°C$) washed for 30 days at 0°C with three changes of amyl acetate.

scanned were changed to the extent evident in Fig.34, but all those viewed showed damage. The fraction epoxidized after the usual washing procedure was found by ^1H NMR analysis to be 0.39 while for two samples washed for 45 days it was 0.37.

Calculations of the average number of monomer units per fold, U, was carried out using equation-3[42] where M_o is the molecular weight of the repeat unit in the polymer and R is the repeat distance per monomer unit along the chain direction in the crystal.

$$U = (L_C/R) \{ (\bar{M}_n/\bar{M}_o) (F_S) - C \} / \{ (\bar{M}_n/\bar{M}_o)(1-F_S) - (L_C/R) \}$$

Equation 3

L_C, the crystal thickness along the chain direction was expressed in terms of the lamellar thickness, L, by the equation[42].

$$L_C = \{ (1-F_S) \rho_A L \} / \{ (1-F_S) \rho_A + F_S \rho_C \}$$ Equation 4

This equation is derived assuming a two phase model for polymer crystallites, with the crystalline thickness, L_C, sandwiched between two noncrystalline portions with total thickness, $L-L_C$. It is further assumed that L_C was directly proportional to the fraction of crystalline material present ($F_C = 1-F_S$) and inversely proportional to ρ_C and $L-L_C$ is directly proportional to F_S and inversely proportional to ρ_A, where ρ_A is the amorphous

density and ρ_c the crystalline density. The lamellar thickness, L, was assumed to be independent of $\bar{M}_n$ and only to depend on T_c. The R value employed (0.439nm) is that given by Takahashi, Sato, Tadokoro and Tanaka[57]; use of the value given by Fisher[56] (0.45nm) would yield U values 5% lower. The value of C the number of monomer units per two chain ends or cilia was found to be negligible in analyzing the results of this experiment and the results for TPI crystallized from concentrated solution[78]. This parameter can be omitted from equation if $\bar{M}_n$ is large and L_c small as is the case for the preparation with $\bar{M}_n$ of 2.9×10^5 . For the preparation with $\bar{M}_n$ of 0.26×10^5, a U value of 6 is found. Use of $1-W_c$ in place of F_s gives U = 9 monomer units per fold. Values of $1-W_c$, L and U are given in Table XVII. Comparison of F_s with $1-W_c$ in Table XVII shows agreement within experimental error at $T_c = 10°C$, where the two preparations used differ by about 30% in molecular weight, near agreement for the samples with $\bar{M}_n$'s of 2.9×10^5 and 0.69×10^5 ($T_c = 20°C$) and a difference of 30% for the preparation with $\bar{M}_n$ of 2.6×10^4 with F_s having smaller value. For the $T_c = 10°C$ preparation F_s slightly exceeded $1-W_c$, therefore $1-W_c$ was used for calculation of U. From the values given in Table XVII a 30% increase in U occurs with about a three-fold change in $\bar{M}_n$ (0.26×10^4 to 0.69×10^4) but no further change is apparent when $\bar{M}_n$ is increased another four-fold. At the highest $\bar{M}_n$ used an increase in U of at least

Table XVII

Noncrystalline Fraction and Number of Monomer Units per Fold for Dilute Solution Grown Trans 1,4 Polyisoprene Crystals

$\bar{M}_n$ x10^{-5}	T_c (°C)	$1-w_c$[a]	L[b] nm	F_s[c]	U[d]
2.1	10	-	-	0.54±.04	-
2.9	10	0.50	7.8	-	8
2.9	20	0.46	9.0	0.41±.02	8
0.69	20	0.48	-	0.43±.02	8
0.26	20	0.44	-	0.33	6
2.9	25	0.46	11.5	-	-
2.9	30	0.44	12.5	≥0.38	≥10
2.9	32	0.44	-	-	-
2.9	34	.43	-	-	-

a. Noncrystalline fraction calculated using density values given in Table VII.

b. Lamellar thickness from electron microscopy.

c. Fraction of monomer units in epoxidized crystals by ^1H NMR.

d. Number of monomer unit per chain fold.

25% takes place when T_C is changed from 10 to 30°C.

A sample of TPI crystallized at 20°C ($\bar{M}_n = 2.9 \times 10^5$) and epoxidized in suspension for 21 days was subjected to ^{13}C NMR analysis in $CDCl_3$ solution. The percentage epoxidation result agrees with the corresponding values obtained by ^1H NMR. Fig.35 and Fig.36 represent the ^{13}C NMR spectra obtained at Bell Laboratories in $CDCl_3$ for TPI reacted in homogeneous $CHCl_3$ solution to 25% and for crystals suspension epoxidized in amyl acetate with MCPBA. The relative intensities of the resonances for the partially epoxidized crystals differ considerably from those for the solution epoxidized sample.

Earlier assignments[79-80] of ^{13}C NMR spectra were based on solution epoxidized TPI only; peak assignments are currently being made with the aid of partially and completely epoxidized squalene samples. Gemmer and Golub[79] interpreted the prominent signals in terms of dyad trans 1,4 units and epoxidized units. Triad sequences were observed for olefinic carbons adjacent to oxirane rings (α , γ , β , δ) as shown below. All the peaks except the peaks with letters P,Q,R,S,T are assigned

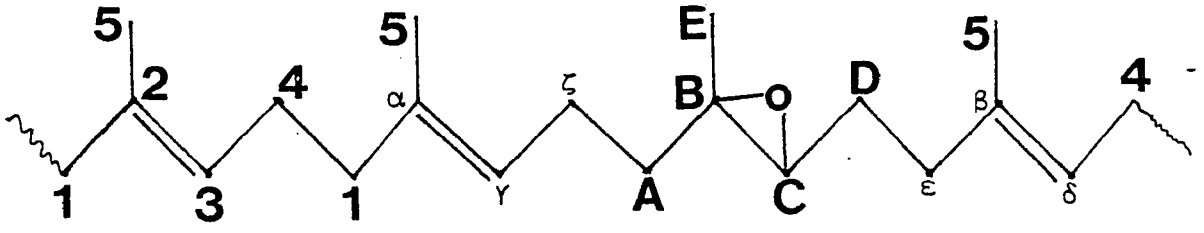

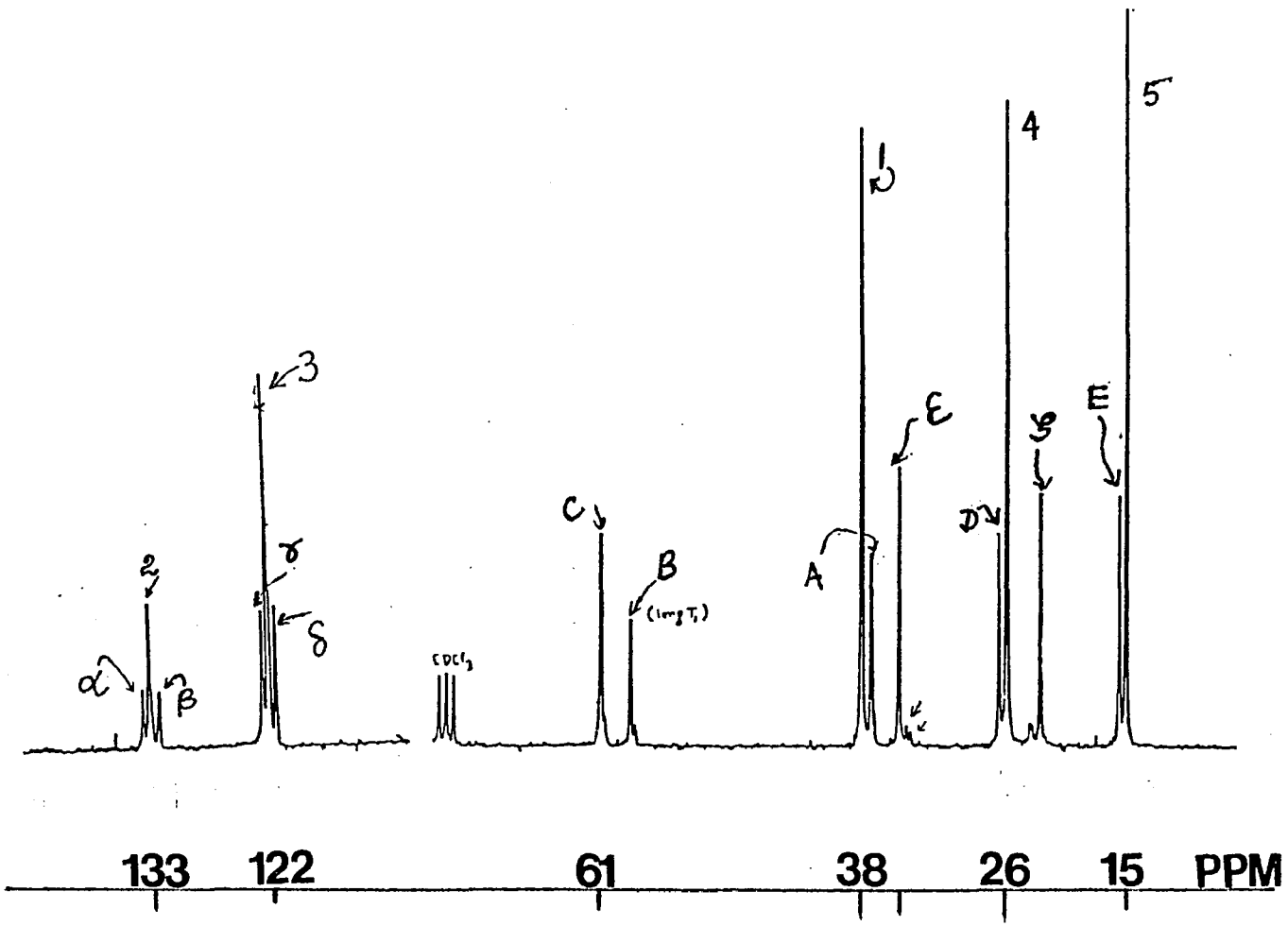

FIG.35 ^{13}C NMR SPECTRUM OF EPOXIDIZED TPI IN $CHCl_3$ SOLUTION.

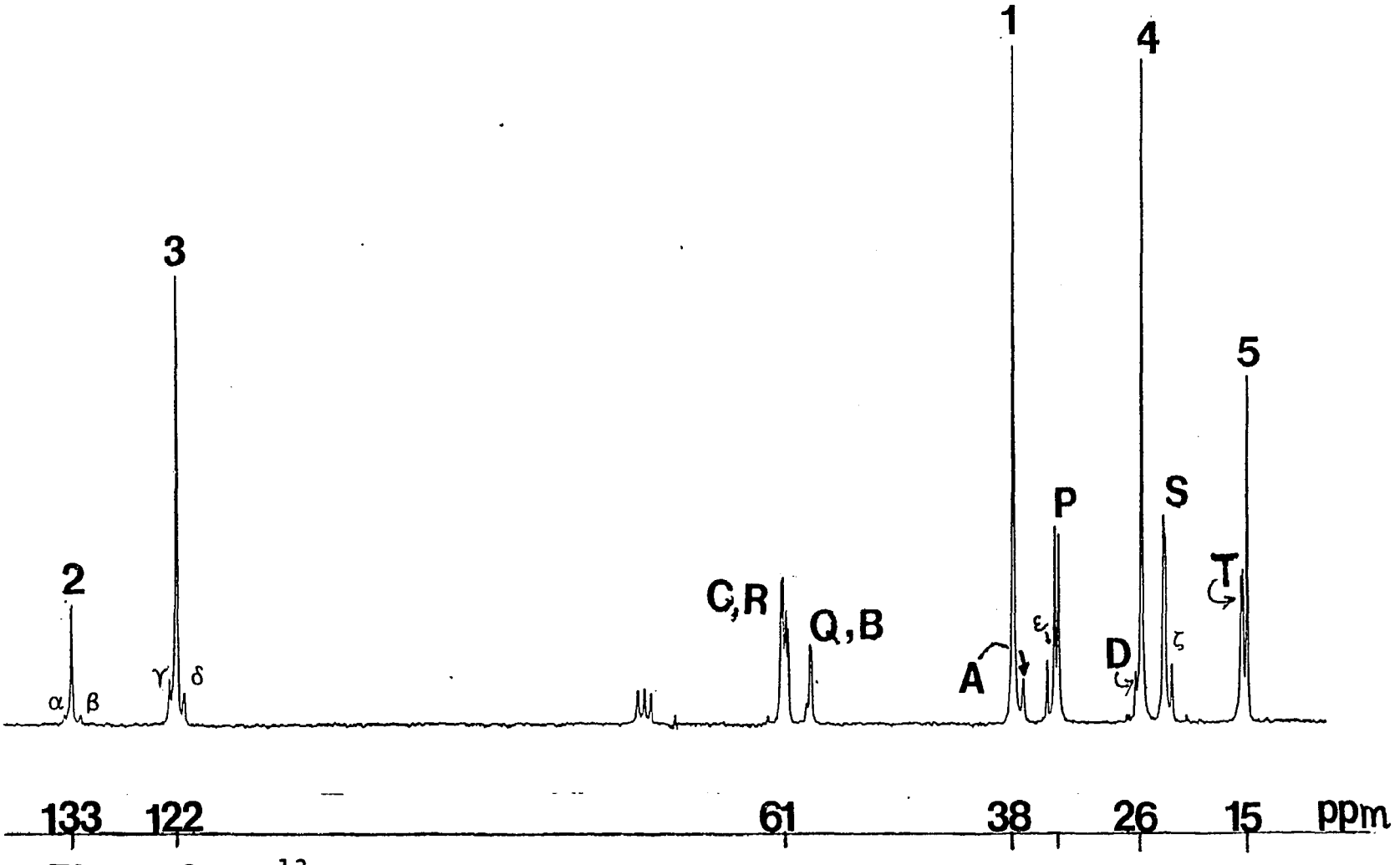

FIG. 36 ^{13}C NMR SPECTRUM OF EPOXIDIZED α TPI CRYSTALS IN AMYL ACETATE SUSPENSION.

with the aid of Gemmer and Golub's or Hayashi et. als[80] interpretation of the solution epoxidized TPI spectra. On comparing the crystal epoxidized spectrum the peaks labelled with letters P,Q,R,S, are not present in the solution epoxidized spectra. Bovey and Schilling have tentatively assigned these peaks as corresponding to the carbons containing adjacent epoxidized isoprene sequence. Also, the splitting observed in these peaks have been interpreted in terms of an oxirane ring chirality, which has also been observed for partially epoxidized TPBD, 3,7-decadiene[81] and squalene. Hayashi et. al have observed an additional peak in between peaks 2 and β, when the extent of epoxidation (in solution) was approximately 40%; this was assigned to carbon 2 surrounded by two epoxidized isoprene units. This peak has not been observed in the crystal epoxidized sample with the same extent of epoxidation. This demonstrates the absence of any isolated unepoxidized isoprene sequences in the crystal sample. The relative peak intensities of bands in the spectra of lamellas epoxidized in suspension differ markedly from those for solution epoxidized samples. In addition the band characteristic of isolated unepoxidized units is absent in the former . These facts can be interpreted as evidence for the presence of relatively long sequences of non epoxidized units followed by epoxidized units. This evidence suggest that the epoxidation reaction is mainly confined to the fold surfaces. The crystal stems and folds of the epoxidized

crystal are represented as given below.

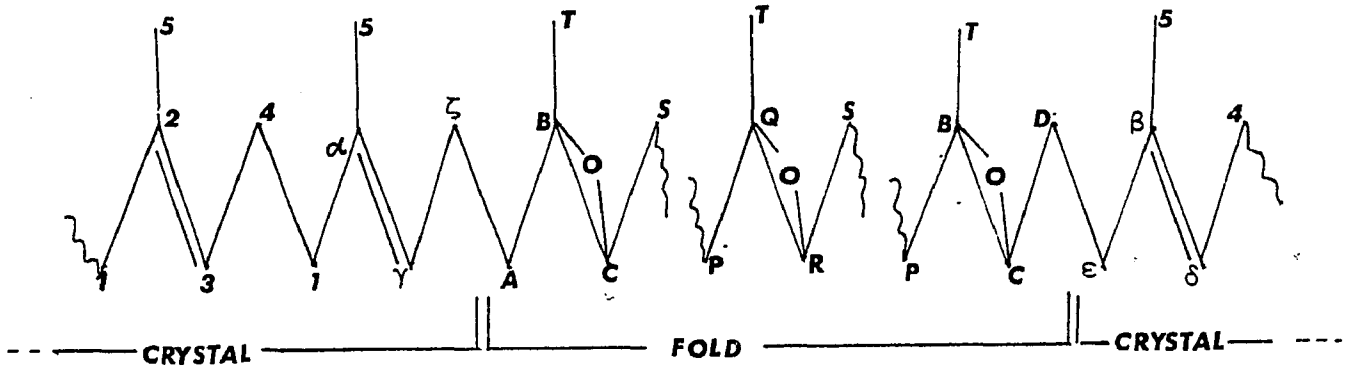

The total resonance area in peak P is taken as proportional to the number of CH_2 carbon atoms present in the fold. (A) represents the area for one of the junction CH_2 carbon atoms and (ϵ) represents the area under the other end of the junction CH_2. The fold length is,

$$U = \{(P/A)+1\} = \{(P/\epsilon)+1\}$$

Assuming heights of the peaks proportional to area, and neglecting any effect due to chain ends, the U value from ^{13}C NMR spectral analysis is 8. This agrees with the value obtained using equations 3 and 4.

The total resonance peak area for the CH_2 carbon atoms in the crystalline stem is taken as proportional to {(I)+(A)}, where I is the area of the resonance due to CH_2 carbon atoms # 1. Then the crystalline stem length is,

$$L_C = \{ (I)+(A) \} / (A) = \{ (I)+(\epsilon) \} / (\epsilon)$$

which yields 59Å; the value obtained using equation 4 is 50Å.

DISCUSSION

Discrimination in terms of solubility differences form the basis of the most widely applicable methods of polymer fractionation. Hence in the column chromatographic technique the success of the fractionation was mainly due to the proper selection of a poor solvent (amyl acetate) and a mild nonsolvent (cellosolve), which is related to the swelling of the precipitate. It is commonly believed that this polymer is sensitive to oxidative changes and this problem was overcome by (I) using an antioxidant (II) using an almost sealed column (III) and passing N_2 during the entire experiment.

One requirement[81] of sucessful fractionation is that the sum of the weight of the fractions should be equal to that of the original weight of the polymer. Some possible explanations for the loss of polymer during the fractionation could be (I) poor coagulation of the lower molecular weight fractions (II) adsorption of the polymer on to the celite surface and, (III) cross-linking of higher molecular weight fractions. The lower molecular weight fractions were recovered in this fractionation (from GPC curves), hence the loss of polymer was caused mainly by (II) and (III).

The crystallization conditions used for most of the preparations in this work[82-83], involving precipitation at 0°C, redissolution at the minimum temperature necessary, T_R, and crystallization at a T_C from 10 to 36°C leads exclusively to the α crystalline form, as determined

by differential scanning calorimetry in all cases and confirmed for some by X-ray analysis. In the absence of precooling and by crystallizing at low temperatures (less than 10°C) mainly the β crystalline form was obtained. The multiple β form endotherms observed on DSC analysis for these preparations suggests that more than one lamellar thickness is present in the final dried product. This could be attributed to either an annealing effect at room temperature in the presence of very small amounts of residual amyl acetate or to non isothermal crystallization caused by the large amount of supercooling. The presence of a very small amount of α form,as determined by DSC, may be also due to the presence of residual solvent. A similar effect was found by Keller et. al[54] when the solvent was changed from dodecane to heptane. This results indicate that the solvent itself has some effect on the stability of the β crystalline form; possibly heptane and amyl acetate may have a greater swelling effect than dodecane, hence converting the β to the α form.

Use of a T_R of 50°C, which is well above the minimum temperature necessary to cause redissolution, yielded a dried sample with the same endotherm temperature as when T_R was 40°C. This was found in the present work[83] by X-ray diffraction to give the α form. However, 50/20°C lamellas have different shapes than the 40/20°C ones ($\bar{M}_n = 2.9 \times 10^5$) and they show only a β electron

diffraction pattern, when precipitated individually , whereas the 40/20°C lamellas show only the α pattern. Therefore, there is a β to α transformation taking place in the 50/20°C crystals when in contact with amyl acetate and/or during the drying process. A β→ α transformation was shown to occur when as received synthetic TPI was swollen at 35°C for 17 hr in amyl acetate[82]. Apparently there is a temperature above which α form nuclei are unstable and therefore cooling from above this temperature leads to crystallization of the β form.

The present results indicate that from dilute solution the form crystallizing is controlled by the following. Crystallization at T_C of 0°C from T_D = 75°C led to β form due to a faster primary nucleation rate. This result is in agreement[65] with the formation of β TPI during melt crystallization. Heating slowly from T_P = 0°C to T_R of 40°C causes transformation of the β form to α form, hence leaving only α nuclei, therefore crystallizing from this temperature (T_R = 40°C) resulted only in the α form. This transformation is probably induced by the lower stability of the β form and a swelling effect at elevated temperatures. Heating well above the redissolution temperature led to destruction of all the existing nuclei, hence crystallizing from T_D of 50°C gave only β form.

Therefore the formation of α and β form during crystallization from dilute solutions are mainly

controlled by the nucleation rate and the swelling of the β form. However for other polymers this temperature mainly controls the number of nuclei, hence regulating the shape and size of crystals[84].

If is found that the regularity of the lamellar faces is a function of molecular weight. Variations of the molecular weight and T_c also has a considerable effect, the higher the $\bar{M}_n$ and the lower T_c, on the tendency to adopt a dendritic habit which usually leads to smaller crystals. In fact the crystal habit and shape offers a rough means of distinguishing between samples of different molecular weights. For polyethylene[85] changing either $\bar{M}_n$ or T_c resulted in two shapes of truncated lozenges. On the other hand for TPI the crystal shape varied from ellipsoidal to hexagonal on decreasing the $\bar{M}_n$ from 10^5 to 10^4 or changing the T_c from 20°C to 30°C. It has been suggested[5] that the truncation is a movement towards equilibrium, because with increasing T_c, and hence with increasing chain mobility, approaching equilibrium was eased. Overgrowths occur as a result of non-isothermal crystallization at lower T_c's.

The increase in the DSC endotherm with increasing T_c reported here[82] is characteristic of lamellar crystals. This is due to the increase in lamellar thickness with an increase crystallization temperature. A similar effect has been reported[59-63] for melt crystallized TPI. The DSC endotherm did not show any observable changes with

$\bar{M}_n$. A small decrease in density was found on changing the $\bar{M}_n$ from $.26 \times 10^5$ - 2.9×10^5. An increase in crystallinity with decreasing $\bar{M}_n$ down to about $\bar{M}_n$ of 10^4 was reported for polyethylene[86-87] and for various polyalkylene oxides[88-91] crystallized from the melt. However at $\bar{M}_n$ below 10^4 a decrease in crystallinity occurs for a number of these polymers, including polyethylene[87] (PE), polyethylene oxide[89] (PEO) and polyhexamethyleneoxide[90] (PHO). Also a decrease in crystallinity with decreasing $\bar{M}_n$ in the 5000-30,000 range was reported[42] for solution crystallized TPBD. For melt crystallized PE [90], PHO[90] and POM[91] a dramatic decrease in basal surface free energy with decreasing molecular weight has been shown. The density variation observed in bulk crystallized polyethylene is explained[92] in terms of the presence of tie molecules or reduced mobility in high molecular weight fractions.

Quantitatively the change in density with $\bar{M}_n$ could be explained using equation 3, rearranged as,

$$(1-F_S) = L_C/R\{1+(U-C)/N\}/\{(U+L_C/R)\}$$

The $(1-F_S)$ values are taken as equal to the crystalline fraction as obtained from density, and N is the degree of polymerization. At large $\bar{M}_n$, $(U-C)/N$ can be neglected; then

$$(1-F_S) = L_C/R\{\ 1/(U+L_C/R)\}$$

At low $\bar{M}_n$, $(1-F_S)$ can change with a change in $\bar{M}_n$; the direction of this change will depend on the relative values of C and U. If C is greater than U then $1-F_S$ decreases as $\bar{M}_n$ decreases (with constant U and L_C/R) as was found for TPBD[42]. The observed increase in crystallinity, W_C, with decreasing molecular weight for α -TPI suggests that the average length of the noncrystallizing chain ends, C/2, is small with respect to U/2, and therefore it can be neglected[78].

Hence $(1-F_S) = L_C/R \{ (1+U/N) \} / \{ (U+L_C/R) \}$

If W_C is used in place of $1-F_S$ assuming a constant L_C, the U values were found to be independent of molecular weight. This means that the increase in density with decreasing molecular weight is due only to that parameter. However the use of epoxidation values for $1-F_S$ lead to a decrease in U with decreasing molecular weight (at constant L_C). The increase in density with T_C at constant $\bar{M}_n$ is mainly controlled by the increase in L_C.

The annealing of the single crystals (α Form) under nitrogen did not produce any appreciable changes in the density or melting point. However thickening of the lamellae along the edges was evident from the electron micrographs. Keller et. al[54] reported a small increase (ca 10 $\mathring{A}$) in the lamellar thickness on annealing the mixture of TPI crystals.

Annealing β -TPI crystals at elevated temperature in the presence of acetone first transforms it to α TPI due to the swelling effect[53]. The presence of an extra endotherm at higher temperature (74°C) indicates that the thickness of this α form is greater than that obtained at 20°C (T-ENDO = 62 - 63°C). When annealing in the dry state up to 55°C α -TPI lamellas grown at 20°C showed no increase in the DSC endotherm. The decrease in density is probably due to the production of long noncrystalline traverses or holes in these converted samples. Another possibility is that during the transformation the crystal melts and recrystallizes leading to a decrease in the density. TPI melt crystallized equal to this annealing temperature exhibits[60] a melting endotherm at 66°C and a crystallinity[60] from density of 0.35 (density of .949g cm^{-3}). This is lower than that for crystals grown from solution at 20°C (crystallinity =.50).

The reaction between diene polymers and a peracid forms the basis of one analytical method for determining the degree of unsaturation in polymers[93-94]. This reaction is a convenient means of introducing epoxide groups into the macromolecules without any side reaction if the reaction is carried out in a non-polar solvent and at very low temperatures[95]. This reaction has been recognized as useful for the modification of natural rubber and thereby producing new rubbers with specialized properties[96]. Depending on the level of

epoxidation, natural rubber yields materials that range from rubbers to hard plastics with improved oil resistance and resistance to ozone cracking.

The kinetics of the epoxidation of peracid with TPI in solution has been shown to be first order with respect to peracid and first order with respect to double bond concentrations[74]. It was found in the present study also, the rate of the reaction of TPI single crystals at the surface depend on both the concentrations of double bonds and peracid (but at higher concentrations extensive damage to the crystals was found).

Dogadkin et. al[74] showed that there are two stages in the epoxidation of squalene with peracid. They concluded that the first stage is evidently due to reaction of the peracid with the more reactive terminal double bonds of squalene, which with the coiled conformation of the squalene molecules are more accessible than the inner double bonds. The second stage corresponds to reaction of the peracid with the inner double bonds. This result is consistent with the data given by Van Duuren and Schmitt[75] on the epoxidation of squalene with peracid. From the epoxidation results of squalene and TPI in chloroform solution Dogadkin et. al further concluded that in solution epoxidation, due to the inductive effect introduced after initial epoxidation, alternative double bonds are the most accessible.

Recently Hayashi et. al[80] have contradicted

the above findings by analyzing the ^{13}C NMR spectra of solution epoxidized TPI and cis-poly butadiene. The spectrum was interpreted in terms of a triad sequence with respect to epoxidized (E) and unepoxidized (I) units. At lower epoxide (19%) content mainly III, IEI triads were found, and at higher epoxide content 40% all the possible triads (III, IEE, IEI, EEE) were found, hence they concluded that the epoxidation reaction is a random reaction and not a selective reaction as proposed by Dogadkin[74] and his coworkers.

While suspended in the solvent the lamellae in the various spiral growths splay, ie are separated from each other except in the vicinity of the screw dislocation[97]. There is little cohesion between the faces of adjacent lamellae. Chemical reactions may take place preferentially at folds for two different reasons; A reaction may be physically confined to fold regions, as for example with a reactant which has only penetrated between polymer lamellae. On the other hand some specific property such as a distorted configuration in the fold region may result in their selection as reaction sites. This latter property has been exploited[98] in studying the development of crystalline texture in melt crystallized TPI, by halting the growth process as a function of time and temperature with OSO_4 staining.

In using a chemical reaction to obtain the fraction of monomer units present at the fold surfaces

in polymer lamellas it is assumed that reaction at the lateral surfaces and in the crystal core is negligibly small. In the present work[83] the lateral surface area is calculated to be approximately 2% or less of the total, depending on the preparation, and therefore the reaction taking place there can be neglected. There was evidence obtained from electron microscopy that during the reaction with MCPBA penetration of the crystal core of TPI lamellas does take place, the severity of this depending on T_c and $\bar{M}_n$ as well as other factors. The observed constancy within experimental error for the double bonds epoxidized at least over part of the reaction time period for four of the five preparations studied suggests that this penetration has only a small effect up to about 20 days reaction time.

Although the general trends in F_s and $1-W_c$ are the same with $\bar{M}_n$ and T_c, there are differences in the values at low $\bar{M}_n$ or high T_c. The surface fraction of TPI crystals ($\bar{M}_n = 2.9 \times 10^5$) has received some study[99] by a bromination reaction and again the general trends found with T_c are the same. However, deviations in the values at $T_c = 30°C$ occurs (F_s is 0.45 from bromination assuming addition to the double bonds only, 0.44 from density and only 0.38 from epoxidation). Comparing the bromination and epoxidation results at higher T_c's it is possible to expect that the epoxidizing agent has not completely

penetrated the amorphous region. However during bromination a certain degree of substitution is expected; hence the difference may be due to this.

It was also found[42] for TPBD lamellas grown from solution that F_s was generally smaller than $1-W_c$. The possible causes for this general behavior were given as (I) the existence of a lower density for the surface fraction as compared to the value extrapolated from the melt thereby causing an error in the crystallinity as calculated from the density. This is in agreement[100-101] with experimental results and calculations for polyethylene, the latter using space filling models and assuming a tight fold. The surface density determined using space filling models for polyethylene was found to change from .65 to .93g cm^{-3} as the number of carbon atoms in the fold ranged from 5 to 19. But the extrapolated melt density was usually taken as 0.86g cm^{-3}. A decrease in amorphous density in equation-1 will considerably increase the crystallinity, (2) the presence[34,102] of partially or totally hidden folds or other defects within the crystal and (3) shielding of the fold surface by absorbed polymer chains[31]. In regard to the latter it was found in the present work that a small decrease in total non-crystalline content does take place when TPI crystals are washed repeatedly over a one to two month period. This suggests that either some desorption or further crystallization occurs. However, it was also found

in this investigation that prolonged washing of epoxidized crystals at 0°C had only a small effect on F_S as determined from the fraction epoxidized although loss of material from the crystal edges was clearly evident. Any polymer chains adsorbed on the crystals are expected to be epoxidized to a high extent. Loss of these chains by desorption and removal during washing should therefore cause a decrease in F_S. Loss of material from the crystal edges should be a slower process and after the first layer is removed should not cause a change in F_S. Since for epoxidized TPI lamellas, F_S shows only a small decrease with extended washing, it is concluded that shielding of the surface by an adsorbed layer does not occur to any appreciable extent.

The largest discrepancies between F_S and $1-W_C$ for TPI appear at lower $\bar{M}_n$. However, the number of hidden folds or defects, if they exist in these lamellas, is expected to decrease with decreasing $\bar{M}_n$. From the limited amount of data available for TPI it is unlikely that the presence of hidden folds or other defects is the principal cause of the differences between F_S and $1-W_C$. Therefore, of the three possible reasons for F_S being less than $1-W_C$ the first one given above is the most likely. The surface fraction, F_S, at a particular temperature for single crystal lamellas should depend mainly upon two factors: the crystalline thickness and the number of monomer units per fold. The lamellar thickness

for various polymers, ie polyethylene[102], TPBD[48] and isotatic polystyrene[103], decreases with decreasing T_c at high temperatures and then becomes invariant. A similar effect was found in this study for TPI also. When the lamellar thickness is increased, F_s should decrease, if the fold length remains constant.

Three different types of folds have been proposed for polymer single crystals.

(I) Irregular adjacent re-entry (loose folds)

(II) Regular adjacent re-entry (tight folds)

(III) Switch board or non-adjacent re-entry folds.

In deciding on the appropriateness of a model it is instructive to calculate the average number of monomer units per fold from the fold region amorphous content, as done in the last section using equation 3.

For a dilute solution grown crystal the surface fraction, F_s, will consist of three components, one due to the folds, another due to noncrystallizing chain ends and the third due to the lateral crystal surfaces. For the crystals investigated the lateral surface area did not exceed 2% of the total surface area and therefore only the first two components are considered. Derivation of equation 3 is as follows. Each chain of degree of polymerization N will have F_s N chain units at the two surfaces and this can be written in terms of the number of monomer units per fold, U, the number of folds per chain, F, and the number of monomer units in the two

noncrystallizing chain ends, C. For a polydisperse system it can be shown the number average D.P., $\bar{M}_n$, should be used, giving the following equation[42].

$$NF_S = \bar{M}_n F_S/M_o = UF+C \quad \text{----------} \quad \text{Equation 5}$$

If it is assumed that the remaining monomer units in the chain, $\bar{N}_n (1-F_S)$ are in the crystalline core, the following equation is obtained:

$$N(1-F_S) = L_C(F+1)/R \quad \text{----------} \quad \text{Equation 6}$$

Where L_C is the crystal thickness along the chain direction, R is the repeat distance in the chain direction and F+1 is the number of chain traverses. Combination of equations 1 and 2 with elimination of F yields equation 3.

W_C values for low molecular weight region of α TPI crystals were calculated[78] using equation 3 assuming a constant U and L_C/R with zero value for C. The U and L_C/R values used were that of a crystal preparation with $\bar{M}_n$ of 1.0×10^5 and $T_C = 20°C$. The W_C's obtained from these assumptions were plotted as a function of $\bar{M}_n$ and compared with W_C's obtained by density measurements. A very good agreement was obtained, hence the assumption of C=0 was justified experimentally.

For TPI the number of monomer units per fold, U, increases with T_C and is possibly smaller at low molecular weight ($\bar{M}_n$ of 2.6×10^4). U values for surface epoxidized

TPBD lamellas with $\bar{M}_n$'s of 1.7×10^4 and 4.4×10^4 have been found[52] using ^{13}C NMR to be 2.4 and 3.0. Therefore at comparable molecular weights the number of monomer units per fold for TPI lamellas (6-10) is about two-fold larger than that for TPBD lamellas. U-values for TPBD fractions were reported[42] to increase with crystallization temperature and to a lesser extent with $\bar{M}_n$, both effects in the same direction as for TPI.

When models [104] of the fold surfaces for α -TPI are constructed using the crystal structures given by Takahashi, Sato, Tadokoro and Tanaka[57] and by Fisher[56] a tight adjacent reentrant fold is found to contain three and four monomer units, respectively, assuming 110 folding[98]. These values are two to three-fold smaller than those found by epoxidation measurement. This therefore suggests that if reentry folding takes place exclusively, then some fold looseness must also occur particularly at higher molecular weights. Another possibility, in agreement with these results, is the presence of some nonadjacent reentry[9] mixed with tight adjacent reentry folding. The number of monomer units per fold necessary to loop over to other than adjacent place will require at least 6-8 monomers if the first adjacent stem is removed and will reguire 9-12 monomers if the first and second adjacent stems are removed. The experimentally obtained values are in the above mentioned range. As discussed earlier the results of this study suggest that

the presence of adjacent reentry folding with an adsorbed noncrystalline over layer is not a viable model.

The method used in this investigation to obtain the number of monomer units per fold depends on the evaluation of a number of parameters including the surface fraction, F_S, the lamellar thickness, L, the monomer repeat distance in the crystal, R, and the amorphous and crystalline densities, ρ_A and ρ_C, respectively. A more direct method of evaluation is preferable. As pointed out above, the average fold length for some trans 1,4-polybutadiene crystal samples have recently been determined[52] using ^{13}C NMR analysis. This method is currently being used to investigate trans 1,4-polyisoprene crystals.

CONCLUSIONS

The following conclusions can be drawn from this investigation:

(1) Sharp molecular weight fractions of TPI could be obtained using the column chromatographic technique with amyl acetate as solvent and cellosolve as nonsolvent at 64°C.

(2) α -TPI single crystals could be prepared from dilute amyl acetate solution by the precooling technique with T_C's in the 10-34°C range.

(3) The dependence of the crystal modification formed on T_R, the redissolution temperature indicates that the formation of α and β TPI in solution is controlled by the primary nucleation rate and swelling effect of the solvent.

(4) Due to the increase in lamellar thickness with increasing T_C the density and the DSC endotherm increased for α -TPI preparations.

(5) A change in the crystal morphology from a hexagonal to an ellipsoidal shape takes place when the molecular weight changes from 10^4 to 10^5.

(6) The fraction of amorphous material on the surface (F_S) of TPI single crystals available for epoxidation by MCPBA is found to depend on $\bar{M}_n$ and T_C.

(7) There are differences in F_S from epoxidation and $(1-W_C)$ obtained by density measurements especially for the lower molecular weight crystal preparation.

However shielding of the surface by adsorbed polymer chains does not occur to any appreciable extent.

(8) The number of monomer units per fold U increases with T_c and is smaller at lower molecular weight.

(9) Results to date suggest that chain folding in TPI crystals consist of nonadjacent reentry folding mixed with tight adjacent reentry folding.

REFERENCES

1) P.H.Till, J.Polym. Sci.; 24, 301 (1957)

2) A.Keller, Phil. Mag., (2) 1171 (1957).

3) E.W.Fischer, Z.Naturforsch, 12a 753 (1957).

4) P.H.Geil, "Polymer Single Crystals" Interscience, New York. (1963).

5) J.Schultz, "Polymer Materials Science" Prentice Hall Inc (1974).

6) E.W.Fischer, R.Lorenz, Kolloid.Z 189, 97 (1963).

7) E.W.Fischer, G.Schmidt, Angew. Chem., 74, 551 (1962).

8) J.B.Jackson, P.J.Flory, R.Chiang, Tran. Faraday Soc 59, 1906 (1963).

9) P.J.Flory, J.Am. Chem. Soc., 84, 2857 (1962).

10) A.Keller, Kolloid.Z. 197, 98 (1964).

11) V.P.Holland, P.H.Lindenmeyer, J.Appl. Phys., 36, 3049 (1965).

12) J.D.Hoffmann, Soc. Plastic Eng., 4, 315 (1964).

13) P.H.Geil, J.Polym. Sci.: 47, 65 (1960).

14) R.J.Roe and H.E.Bair, Macromolecule, 3, 454 (1970).

15) A.Keller, E.Martuscelli, D.J.Priest and Y.Udagawa, J.Polym. Sci. A2 10, 1807 (1971).

16) R.J.Roe, J.Chem. Phys., 53, 3026 (1970).

17) L.Mandelkern, J.Polym Sci.: Polym Revs. 50, 457 (1975) Acc. Chem. Res. 9, 8 (1976).

18) I.R.Harrison, J.Runt, L.J.Stanislow and D.A.Bell, J.Polym. Sci.: Polym. Phys. Ed. 17, 63 (1979).

19) K.H.Illers and G.Kanig Colloid and Polymer, Sci.: 260, 564 (1982).

20) J.F.Jackson, L.Mandelkern, Macromolecule, 1, 547 (1968).

21) M.I.Bank and S.Krimm, J.Polym. Sci.: A2 7, 1785 (1969).

22) T.C.Cheam and S.Krimm, J.Polym. Sci.: Phys Ed 19, 423 (1981).

23) F.C.Stehling, E.Ergos and L.Mandelkern Macromolecules 4, 672 (1971).

24) Xiabin Jing, and S.Krimm. J.Polym. Sci.: Polym. Phys. Ed. 20, 1155 (1982).

25) R.Voekel and H.Sillescu, Macromol. 12, 162 (1979).

26) Y.Udagawa and A.Keller, J.Polym. Sci.: A2 9, 437 (1971).

27) E.Ergoz and L.Mandelkern. 10, 631 (1972).

28) D.J.Blundell, A.Keller and T.M.Connor, J.Polym. Sci.: A2 5, 991 (1967).

29) E.W.Fischer and A.Peterlin, Makromol. Chem. 74, 1 (1964).

30) K.Bergmann and K.Nawotki, Kolloid Z.U.Z.Polymers 250, 1094 (1972).

31) J.D.Hoffman, G.T.Davis, J.Res. Natl Bur. Stand Sec, A 79A, 613 (1975).

32) A.Keller and Y.Udagawa, J.Polym. Sci.: A2 9, 1793 (1971).

33) D.J.Priest, J.Polym. Sci.: A2 9, 1777 (1971).

34) G.N.Patel and A.Keller, J.Polym. Sci.: Polym. Phys. Ed 13, 2259 (1975).

35) A.Keller, W.Matreyek and F.H.Winslow, J.Polym. Sci.: 62, 291 (1962).

36) I.R.Harrison and E.Baer, J.Polym. Sci.: A2 9, 1305 (1971).

37) M.Eguiluz, H.Ishida and A.Hiltner, J.Polym. Sci.: Polym. Phys. Ed. 17, 893 (1979); 18, 2295 (1980).

38) I.R.Harrison, J.S.Butler and J.P.Runt, Org, Coatings and Plastics Chem. Reprints 44, 176 (1981).

39) J.Guzman, J.G.Fatou and J.M.Perena, Makromol. Chem 181, 1051 (1980).

40) P.Wichacheewa and A.E.Woodward,J.Polym. Sci.: Polym. Phys. Ed 16, 1849 (1978).

41) J.M.Stellman and A.E.Woodward, J.Polym. Sci.: B7 755 (1969); A2 9, 59 (1971).

42) S.Tseng, W.Herman, A.E.Woodward and B.A.Newman Macromolecules 15, 338 (1982).

43) T.Tatsumi, T.Fukushima, K.Imada and M.Takayanagi, J.Macromol. Sci-Phys. B1, 459 (1967).

44) C.Hendrix, D.A.Whiting and A.E.Woodward, Macromolecules 4, 571(1971).

45) H.Evans and A.E.Woodward, Macromolecules 9, 88 (1976).

46) S.B. Ng, J.M.Stellman and A.E.Woodward, J.Macromol Sci-Phys. B7, 533 (1973).

47) A.Marchetti and E.Martuscelli, J.Polym. Sci.: Polym Phys. Ed. 14, 323 (1976)

48) J.Finter and G.Wegner. Makromol. Chem 182, 1859 (1981),

49) B.Newman, J.M.Stellman and A.E.Woodward. J.Polym Sci.: Polym. Phys. Ed. 19, 2311 (1972).

50) A.Marchetti and E.Martuscelli J.Polym. Sci.: Polym. Phys. Ed. 14, 151 (1976).

51) S.B Eng and A.E.Woodward, J.Macromol. Sci-Phys. B10, 627 (1974).

52) F.C.Schilling, F.A.Bovey, S.Tseng and A.E.Woodward Macromolecules 16, 808 (1983).

53) W.Schlesinger and H.M.Leeper, J.Polym. Sci.: 11, 307 (1953).

54) A.Keller and E.Martuscelli, Makromol, Chem. 151, 189 (1972).

55) C.W.Bunn, Proc. Roy. Soc. (London) A180, 40 (1942)

56) D.Fisher, Proc. Phys. Soc. (London) 66, 7 (1953).

57) Y.Takahashi, T.Sato, H.Tadokora and Y.Tanaka, J.Polym. Sci.: Polym. Phys. Ed. 11, 233 (1973).

58) L.Mandelkern, F.A.Quinn, Jr., and D.E.Roberts, J.Am. Chem. Soc. 78, 926 (1956).

59) R.D.Flanagan and A.M.Rijke, J.Polym Sci.: A-2, 10, 1207 (1972).

60) W.Cooper and G.Vaughan, Polymer, 4, 329 (1963).

61) H.M.Rootare and J.M.Powers, J.Dent, Res., 36, 1453 (1977).

62) E.G.Lovering and D.C.Wooden, J.Polym. Sci.: A-2. 7, 1639 (1969).

63) E.G.Lovering and D.C.Wooden, J.Polym. Sci.: A-2, 9, 175 (1971).

64) G.Schuur, J.Polymer. Sci.: 11, 386 (1953).

65) E.Fischer and J.F.Henderson, J.Polym. Sci.: A-2, 5, 377 (1967).

66) B.C.Edwards, J.Polymer. Sci.: polym. Ed. 13, 1387 (1975).

67) P.J.Phillips, D.Sorenson J.Polymer Sci.: Polymer Lett. Ed. 19, 585 (1981).

68) H.L.Wagner and P.J.Flory, J.Am Chem. Soc. 74, 195 (1952).

69) W.Cooper, D.E.Eaves and G.Vaughan. J.Polym. Sci.: 59, 241 (1962).

70) E.G.Lovering and W.B.Wright, J.Polym. Sci.: A-1, 6, 2221 (1968).

71) E.G.Lovering, J.Polym. Sci.: Part C, 30, 329 (1970).

72) J.F.Henderson and J.M.Hume, J.Appl. Polym. Sci.: 11, 2349 (1971).

73) P.M.Henry, J.Polym. Sci.: 36, 3. (1959).

74) I.A.Tutorskii, I.D.Khodzhaeva and B.A.Dogadkin, Polym. Sci.: USSR 16, 186 (1974).

75) B.L.Van Duuren and F.L.Schmitt, J.Org. Chem. 25, 1761 (1960).

76) R.G.Carlson, N.S.Behn, C.J.Cowles, J.Org. Chem 36, 3832 (1971).

77) P.T.Poluektov, T.B.Gonsovskaya, F.G.Ponomarev and Yu.K.Gusev, Vysokomol. Soyed., A15, (3) 606 (1973).

78) C.C.Kuo and A.E.Woodward to be published.

79) R.V.Gemmer and M.A.Golub, J.Polym. Sci.: Polym. Chem. 16, 2985 (1978).

80) O.Hayashi, T.Takahashi, H.Kurihara and H.Uene, Polym.J 13, 215 (1981).

81) M.J.R.Cantow,Ed,"Polymer Fractionation" Academic press Inc NY (1966).

82) K.Anandakumaran, C.C.Kuo, S.Mukherji and A.E.Woodward. J.Polymer Sci.: Polym. Phys. 20, 1669 (1982).

83) K.Anandakumaran, W.Herman and A.E.Woodward. Macromolecules 16, 563 (1983).

84) D.J.Blundell, A.Keller and A.J.Kovacs J.Polymer. Sci.: B4, 481 (1966).

85) D.C.Bassett and A.Keller Phil. Mag. 7, 1553 (1962).

86) F.Hamada, B.Wunderlich, T.Sumida, S.Hayashi, A.Nakajima, J.Phys, Chem. 72, 178 (1968).

87) W.Banks, M.Gordon, R-J.Roe, A.Sharples, Polymer 4, 61 (1963).

88) J.Q.G.Maclaine, C.Booth, Polymer 16, 680 (1975).

89) K.Se, K.Adachi, T.Kotaka, Polymer.J 13, 1009 (1981).

90) C.Marcro, J.G.Fatou, A.Bello. Polymer 18, 1100 (1977).

91) C.Marcro, J.G.Fatou, A.Bello, A.Blanco. Polymer. 20, 1250 (1979).

92) J.D.Hoffman, G.Thomas Davis and J.I.Lauritzen Treatise on solid state Chemistry Vol3, Plenum NY . Ed, N.B.Hannay. (1976).

93) I.M.Kolthoff, T.S.Lee and M.A.Mairs. J.Polym. Sci.: 2, 199 (1947).

94) I.M.Kolthoff and T.S.Lee. J.Polym. Sci.: 2, 226 (1947).

95) C.E.Wheelock, Ind. Eng. Chem. 50, 299 (1950).

96) P.W.Allen"Plastics and Rubber International". 7, 49 (1982).

97) P.H.Geil."Introduction to Polymer Science and Technology" Ed H.S.Kaufman and J.J.Falcetta, Inter science NY (1978).

98) C.K.L.Davies and O.E.Long, J.Mat. Sci.: 12, 2165 (1977).

99) M.Taylor and A.E.Woodward, Unpublished results.

100) I.R.Harrison and J.Runt, J.Macromol. Sci.: Phys. B17, 83 (1980).

101) I.R.Harrison and T.Juska, J.Polym. Sci.: Polym. Phys. Ed. 17, 491 (1980).

102) B.Wunderlich, Macromolecular Physics, Vol.1. Academic Press (1973).

103) D.H,Jones, A.J.Latham, A.Keller and M.Girolamo, J.Polym. Sci.: Polym. Phys. 11, 1759 (1973).

104) S.Mukherji, Unpublished results.